https://doi.org/10.5194/egusphere-2026-2005
Preprint. Discussion started: 28 April 2026

Assessing the plausibility of unprecedented events: A process-based approach applied to month-long heatwaves in Western Europe

Florian E. Roemer[1], Erich M. Fischer[1], Robin Noyelle[1], and Reto Knutti[1]

[1]Institute for Atmospheric and Climate Science, ETH Zürich, Zürich, Switzerland

Correspondence: Florian E. Roemer (florian.roemer@env.ethz.ch)

Abstract. Climate model based storylines of individual climate and weather events are increasingly used to quantify impacts, vulnerability, or stress-test infrastructure to inform adaptation decisions. Here, we present an approach to test the plausibility of unprecedented climate storylines based on physical conformity, internal consistency, and historical precedent. We apply this approach to assess the plausibility of month-long heatwaves in Western Europe that would exceed existing record temperatures by around 5 K. These heatwaves are based on model simulations using ensemble boosting, a computationally efficient method to simulate unprecedented events. We compare these unprecedented heatwaves with historical heatwaves in a reanalysis data set, using standardised anomalies relative to a time-evolving climatology of relevant physical variables such as temperature, 500 hPa geopotential height, surface solar radiation, and soil moisture. We show that these unprecedented heatwaves are associated with physical drivers similar to historical heatwaves, with anomalies that are more intense in magnitude but very similar in their temporal substructure. We also demonstrate that the relationships between different physical variables are internally consistent and exhibit many similarities with historical precedents. In this way, we show that these unprecedented long-lasting heatwaves cannot be ruled out as implausible, and thus highlight the need to anticipate such events when planning adaptation measures. Similar approaches can be used to assess the plausibility of unprecedented events in other variables.

1 Introduction

Unprecedented events represent a particularly difficult challenge for extreme event research: It is essential to study them for disaster preparedness, but their rare occurrence in observational records limits our ability to make robust statements regarding their potential magnitude and characteristics (Fischbacher-Smith, 2010; Kelder et al., 2025). Unprecedented events can be simulated in climate models, but the lack of historical analogues of comparable magnitude leads to the fundamental question whether these simulated events are plausible to occur in the real world. This question is particularly pressing following the record-shattering 2021 Pacific North West heatwave that broke previous temperature records by almost 5 K, which has highlighted the importance of anticipating future unprecedented events (Bartusek et al., 2022; White et al., 2023; Fleishman et al., 2025). Here we assess the plausibility of simulated month-long heatwaves in Western Europe that would exceed existing records by similar margins (Lüthi et al., 2024).

Future record-breaking events can be studied using climate storylines, which provide physically self-consistent unfoldings of plausible future events, making it possible to study their characteristics and underlying physical processes (Hazeleger et al.,

https://doi.org/10.5194/egusphere-2026-2005
Preprint. Discussion started: 28 April 2026

2015; Shepherd et al., 2018; Sillmann et al., 2021; Baulenas et al., 2023; van den Hurk et al., 2023; Baldissera Pacchetti et al., 2024). Among other approaches, such unfoldings of future events can be selected from single-model initial-condition large ensembles (SMILEs) of climate models (Bador et al., 2017; van der Wiel et al., 2021; Suarez-Gutierrez et al., 2020; Fischer et al., 2021) or from ensembles of weather prediction models (UNSEEN approach, van den Brink et al., 2005; Thompson et al., 2017). Furthermore, model ensembles can be optimised to simulate more frequent and intense extreme events by using rare event algorithms such as the GKTL algorithm (Giardina et al., 2011; Ragone et al., 2018; Ragone and Bouchet, 2021; Yiou et al., 2023; Noyelle et al., 2025a, b), ensemble boosting (Gessner et al., 2021; Fischer et al., 2023; Lüthi et al., 2024; Suarez-Gutierrez et al., 2025), or based on adaptive multilevel splitting (Finkel and O'Gorman, 2024, 2026). In recent years, similar approaches have been used to create extreme event storylines using machine learning (Mahesh et al., 2025a, b; Whittaker and Di Luca, 2026). However, for all of these approaches, an important question remains: How can we test whether simulated unprecedented events are plausible to occur in the real world?

Assessing the plausibility of unprecedented events is essential because it informs us about the potential intensity of events that society needs to prepare for (Nordmann, 2013). This makes plausibility an essential criterion for decision making, such as for natural disaster preparations (van der Helm, 2006; Shepherd et al., 2018; Sillmann et al., 2021). Located between the possible (without contradiction) and the probable (likely to occur), the plausible is associated with being credible, trustworthy, and reasonable (Amara, 1991; Wilson, 1998; Selin, 2006; van der Helm, 2006; Nordmann, 2013; Urueña, 2019). However, the concept of plausibility is based on subjective judgement, and thus there are no universal criteria (Selin and Guimarães Pereira, 2013). In this work, we base our assessment of plausibility on tangible criteria that are suitable to evaluate climate storylines: conformity with physical principles, internal consistency, and historical precedent (Amara, 1991; Nordmann, 2013).

There are a number of different ways to translate plausibility criteria into concrete analysis steps. Most commonly, the plausibility of simulated extremes is statistically analysed through extreme value theory and model fidelity tests (Thompson et al., 2017, 2019; Vautard et al., 2019; Philip et al., 2020; Kelder et al., 2022a, b). In contrast, only few studies assess the plausibility of simulated extreme events by analysing the physical processes that drive them (Vautard et al., 2019; Kelder et al., 2022b). An important part of this assessment involves comparisons with historical events; however, there are inherent limitations of this approach when analysing unprecedented extremes in a transient climate. This is particularly obvious for extreme events that are directly affected by global and regional warming trends; for example, heatwaves that reach previously impossible temperatures are becoming possible in a warming climate (Fischer et al., 2025). To account for this, we propose a process-based approach centred around standardised anomalies with respect to a time-evolving climatology, that is, we quantify how extreme an event is relative to the background climate (mean and variability) in which it occurs. Expanding on existing process-based studies, this allows us to directly and systematically compare anomalies in a wide range of physical drivers during simulated unprecedented events with anomalies during historical heatwaves and to evaluate their consistency with current process understanding.

To demonstrate our approach, we focus on heatwaves in Western Europe. This is motivated by the fact that both mean summer temperatures and extreme heat in Western Europe are increasing faster than in almost any other region, caused by a combination of global anthropogenic climate change, reductions in aerosol emissions, and changes in circulation (Singh

https://doi.org/10.5194/egusphere-2026-2005
Preprint. Discussion started: 28 April 2026

et al., 2023; Vautard et al., 2023; Schumacher et al., 2024; World Meteorological Organization (WMO) et al., 2025). As a consequence, Western Europe has been a hotspot for record-breaking heat extremes: Since the turn of the 21st century, Western Europe experienced record-breaking heat extremes in 2003, 2006, 2015, 2018, 2019, 2022, and most recently in 2025 (Rebetez et al., 2009; García-Herrera et al., 2010; Russo et al., 2015; Kornhuber et al., 2019; Sánchez-Benítez et al., 2022; Feser et al., 2024; Hotz et al., 2024; Copernicus Climate Change Service, 2025). Given current global warming trends, the likelihood of record-breaking heatwaves is expected to increase further in the future (Fischer et al., 2025), with parts of Western and Central Europe among the most at-risk regions for such events (Thompson et al., 2023).

The processes that govern heatwaves occur on a wide range of spatial and temporal scales and include interactions between the atmosphere, ocean, cryosphere, land surface, and biosphere (Barriopedro et al., 2023; Domeisen et al., 2023). In mid-latitudes, heatwaves are often caused by quasi-stationary Rossby wave packets that lead to persistent anticyclones (Röthlisberger et al., 2019). These anticyclones can disrupt the zonal atmospheric circulation leading to atmospheric blocking (Drouard and Woollings, 2018; Röthlisberger and Martius, 2019; Kautz et al., 2022). In summer, this can favour heat extremes through horizontal temperature advection, vertical adiabatic subsidence, and diabatic heating at the surface through solar radiation and turbulent fluxes, which are often amplified by land-atmosphere feedbacks (Fischer et al., 2007; Seneviratne et al., 2010; Zschenderlein et al., 2019; Barriopedro et al., 2023; Röthlisberger et al., 2025). These generally well-understood physical drivers provide the foundation for our process-based approach to assess plausibility.

Heatwaves have severe impacts on human health, ecosystems, and infrastructure (Easterling et al., 2000; Zuo et al., 2015), and these impacts can be particularly severe during persistent heatwaves lasting multiple weeks (D'Ippoliti et al., 2010; Anderson and Bell, 2011; Polt et al., 2023). Compared with short-lived heatwaves, long-lasting heatwaves in Western Europe tend to be associated with particularly strong low-wavenumber Rossby wave trains and land-atmosphere feedbacks (Tuel and Martius, 2023; Pappert et al., 2025). Prominent examples of long-lasting heatwaves include the Eastern European heatwave of 2010 (Barriopedro et al., 2011; Dole et al., 2011) as well as the Western European heatwaves of 1976 (Green, 1977; Rodda and Marsh, 2011; Kendon et al., 2024) and 2003 (Black et al., 2004; García-Herrera et al., 2010), which resulted in thousands of excess deaths (Le Tertre et al., 2006; Robine et al., 2007).

Recent model experiments based on ensemble boosting suggest that persistent, month-long heatwaves that would break observational records by more than 5 K in Western Europe are possible in the near future, which would have severe effects on heat-related mortality (Lüthi et al., 2024). Given the unprecedented nature of these month-long heat extremes, here we address the pressing question whether they are plausible to occur in the real world.

2 Methods

2.1 Climate model and reanalysis data

The unprecedented heatwave storylines are created using ensemble boosting, a computationally efficient method to simulate record-breaking extremes using the CESM2 climate model (Gessner et al., 2021). It consists of re-initialising a model run a few weeks before an extreme event and creating new ensembles based on round-off sized perturbations in the humidity

https://doi.org/10.5194/egusphere-2026-2005
Preprint. Discussion started: 28 April 2026

Table 1. Heatwave characteristics and drivers analysed in this study.

TM	daily mean temperature
TX	daily maximum temperature
TN	daily minimum temperature
Z500	500 hPa geopotential height
U500	500 hPa zonal wind (positive eastwards)
V500	500 hPa meridional wind (positive northwards)
ω500	500 hPa vertical wind (positive downwards)
SSR	surface downwelling solar flux (positive downwards)
PREC	total precipitation
SM	top-layer soil moisture
LHF	surface latent heat flux (positive upwards)
SHF	surface sensible heat flux (positive upwards)
EF	surface evaporative fraction

field. The simulations used here are based on a 35-member CESM2 ensemble running from 2005 to 2035 under the historical (2005–2014) and SSP3-7.0 (2015–2035) scenarios (Fischer et al., 2023; Lüthi et al., 2024). From this ensemble, the five most extreme 14-day heat extremes in Switzerland ("parents") were selected, occurring in the model years 2015, 2028, 2028, 2030, and 2031 in different ensemble members. For each parent, 100 ensemble members per day start 14–25 days before the peak of the parent event and subsequently run for 50 days, yielding a total of 1100 alternative realisations of each parent heatwave. These simulations were already used and described by Lüthi et al. (2024).

As a climatological reference for these boosting simulations, we use the 100-member CESM2 large ensemble (LE) that runs from 1850 to 2100 under historical (1850–2014) and SSP3-7.0 (2015–2100) scenarios (Danabasoglu et al., 2020; Rodgers et al., 2021). We use a number of atmospheric and surface variables, most of which are directly available as model output (see Tab. 1). The exceptions are total precipitation (PREC), which is calculated as the sum of convective precipitation (PRECC) and large-scale precipitation (PRECL), and the evaporative fraction (EF), which is calculated from surface latent (LHF) and sensible heat fluxes (SHF) as $\mathrm{EF} = \mathrm{LHF}/(\mathrm{LHF} + \mathrm{SHF})$.

To compare with historical heatwaves, we use the ERA5 reanalysis for the years 1950–2024 (Hersbach et al., 2020) for all variables in Tab. 1 except for SM, for which we use ERA5-Land instead (Muñoz-Sabater et al., 2021). For SM, the top-layer of the soil differs between CLM, CESM2's land model (top 10 cm) and ERA5-Land (top 7 cm). To test the impact of this difference and the choice to focus on the top-layer only, we also perform our analysis for the top 1 m of the soil. This slightly changes some of our results quantitatively but does not alter any of our conclusions. In the following, we therefore focus only on the soil moisture of the top-layer (SM).

In our analysis, we focus on a box in Western Europe where the boosting simulations described above detect potential heatwaves that would exceed existing observational records by particularly large margins (0–10°E, 46–51°N, covering North-

https://doi.org/10.5194/egusphere-2026-2005
Preprint. Discussion started: 28 April 2026

Eastern France, South-Western Germany, Switzerland, Belgium, Luxemburg, and Liechtenstein; referred to as WE in the following). All CESM2 and ERA5 variables are averaged over this domain before we calculate standardised anomalies (see below). To study large-scale conditions, we further use the full horizontal fields of all variables analysed in Europe (12°W – 42° E, 35°N – 72°N). For this analysis, we remap the horizontal ERA5 fields to the CESM2 grid using first order conservative remapping (Schulzweida, 2023). Unless stated otherwise, all of our analysis is performed for the summer months of June, July, and August (JJA).

2.2 Standardised anomalies

To allow for a meaningful comparison between the simulated unprecedented heatwaves from the CESM2 boosting simulations and historical heatwaves from ERA5, we express every variable x in terms of standardised anomalies z_x (in the following referred to as "anomalies" for brevity):

$$z_x(r,y,s) = \frac{x(r,y,s) - \overline{x}(r, y \pm 15\,\mathrm{yr}, s \pm 2\,\mathrm{d})}{x'(r, y \pm 15\,\mathrm{yr}, s \pm 2\,\mathrm{d})}. \tag{1}$$

Here, the region r refers to an individual grid cell (after remapping) or the box-average over WE, y refers to the year, s refers to the day of the summer season (JJA), and $\overline{x}$ and x' refer to the mean and standard deviation of x, respectively, calculated over a centred 31-year window in time and a centred 5-day window over the seasonal cycle.

For the boosting simulations, $\overline{x}$ and x' are derived from the CESM2-LE, using all 100 ensemble members for the 31-year period centred on each heatwave. The only exception is the SM variable, which is available for only 90 members of the ensemble. For the CESM2-LE itself, the standardisation is performed for the period 2005–2035 (the same period as the 35-member CESM2 ensemble on which the boosting simulations are based), using model output from the period 1990–2050. For ERA5, the standardisation is limited to the period 1965–2009 where a centred 31-year reference period can be constructed based on the data record available at the time of the analysis (1950–2024). When LHF and SHF are of opposite sign but similar magnitude, this can lead to very large absolute values in EF locally, particularly over ocean. Thus, only grid cells with an EF value between 0 and 1 are used to calculate EF anomalies.

The standardisation is performed separately for daily values and a 30-day running mean. The 30-day running mean is assigned to the "central day", the 15th day within the 30-day period. We consider all 30-day periods whose central day lies in JJA, including those that start in May or end in September. To calculate the 30-day running mean of the box-mean over WE, we require data points on all 30-days within a given window; for the running mean of individual grid points, this is relaxed to at least 25 data points within a 30-day window in order to reduce the effect of individual missing values in EF (see above).

2.3 Event selection

Based on the anomalies in the 30-day running mean of TM, we select the ten most extreme 30-day heatwaves in WE in our boosting simulations ("unprecedented" heatwaves U1–U10, Tab. A1) as well as in ERA5 ("historical" heatwaves H1–H10, Tab. A2). In order to only select non-overlapping time periods, in the boosting simulations, we only consider the maximum 30-day anomaly of each boosting run; in ERA5, we only consider the maximum 30-day anomalies within $\pm 30\,\mathrm{days}$. In this way,

https://doi.org/10.5194/egusphere-2026-2005
Preprint. Discussion started: 28 April 2026

we select the 30-day periods that feature the most anomalously high temperatures with respect to the background climate and the timing within the summer season in which they occur. Of the ten selected unprecedented heatwaves, eight come from the same parent heatwave ensemble in model year 2015 (P1), and the other two (U4 and U8) come from a second parent heatwave ensemble in model year 2031 (P2). Nevertheless, they are still quite distinct in terms of their TM time series (Fig. A1) and their physical drivers (Sect. 3.2).

To directly compare the historical heatwaves to CESM2 heatwaves of similar magnitude, we additionally select "moderate" heatwaves in CESM2. For each historical heatwave (H1–H10), we select the 20 heatwaves in the CESM2-LE with the most similar 30-day TM anomaly over WE. In this way, we select a total of 200 moderate CESM2 heatwaves whose TM anomalies differ from the respective historical heatwave by at most $\pm 0.1\,\sigma$ (Fig. 1a).

2.4 Return periods

To estimate the return periods of the unprecedented heatwaves from the ensemble boosting simulations, we use a method that was specifically developed for this purpose and is described in detail by Bloin-Wibe et al. (2025). In short, this method uses the shared antecedent conditions between a boosted simulation and its parents to derive conditional probabilities of exceeding a threshold $\mathrm{TM}_{\mathrm{ref}}$ and uses bootstrapping to derive the 95 % confidence interval of the estimated return period. It provides an unbiased estimate of return periods and offers clear improvements over approaches based on fitting extreme value distributions.

When applying this method to our simulations, it should be noted that the parent heatwaves were selected based on the 14-day absolute TM in Switzerland, while our study considers the 30-day TM anomaly in WE. As a consequence, the five selected parent heatwaves are not among the most extreme heatwaves in the ensemble; rather, they are ranked 16th, 23rd, 133rd, 265th, and 294th in terms of their 30-day TM anomaly in WE (out of the 35 ensemble members · 31 ensemble years = 1085 simulated years; see Fig. 1b). Thus, setting $\mathrm{TM}_{\mathrm{ref}}$ equal to the least extreme parent run, the antecedent conditions are sampled less efficiently than is theoretically possible, but, importantly, this does not affect the quality of the return period estimator. Return periods of heatwaves in the 35-member ensemble (including parent heatwaves) are estimated using an empirical frequency estimator based on the occurrence within the ensemble (Bloin-Wibe et al., 2025).

The ten selected unprecedented heatwaves are from ensemble members that are re-initialised 11–20 days before the peak of the 30-day TM anomaly in WE in the parent run and thus we use all ensemble members with lead times of 11–20 days to estimate conditional probabilities. Note that these lead times do not correspond directly to the lead times defined with respect to the 14-day TM in Switzerland in Sect. 2.1. All days of the ten most extreme 30-day periods (U1–U10) occur after the re-initialisation, and thus do not include any simulated days from the respective parent simulation.

2.5 Temporal substructure

To compare the temporal substructures of U1–U10 with H1–H10, we use daily anomalies of the variables listed in Tab. 1. For each variable, these daily anomalies within each 30-day period are ranked from highest to lowest, similar to the approach used by Röthlisberger et al. (2020). To evaluate systematic differences, the ranked anomalies are averaged over the ten historical and ten unprecedented heatwaves, as well as the selected moderate heatwaves from the CESM2-LE, respectively.

https://doi.org/10.5194/egusphere-2026-2005
Preprint. Discussion started: 28 April 2026

We evaluate the persistence of TM, Z500, U500, and SM by calculating the number of consecutive days in which the daily anomalies are greater than $+1\,\sigma$ (for TM and Z500) or less than $-1\,\sigma$ (for U500 and SM). For ERA5 and the CESM2-LE, we consider periods of consecutive days whose end date lies in JJA, including periods that start in preceding months, and divide their occurrences by 92 (the number of days in JJA) to yield their frequency per summer season. For the simulated unprecedented heatwaves, we take the longest persistence period that ends in the 50-day period of each boosting run, including periods that start in their respective parent run. Thus, persistence periods from all sources can include days from months preceding JJA.

2.6 Multivariate linear model

To test the plausibility of U1–U10 from a multivariate perspective, we construct a simple multilinear statistical model based on a multivariate ordinary least-squares regression. For simplicity, we focus on a set of five predictors (Z500, U500, V500, SM, SSR) and apply it separately for three different prognostic variables (TM, TX, and TN). For each prognostic variable separately, the model is fitted to the maxima of 30-day z_{TM} of each summer season (JJA), with separate versions trained on ERA5 and the CESM2-LE. This gives six different model versions which are used to infer anomalies in the prognostic variable during the unprecedented heatwaves based on the simulated anomalies of the five predictors as

$$z_{x,\mathrm{inf}}(d) = \sum_{p} \beta_p \, z_p. \tag{2}$$

Here, $x \in$ [TM, TX, TN] is the prognostic variable, $p \in$ [Z500, U500, V500, SM, SSR] are the predictors, $d \in$ [CESM2-LE, ERA5] are the data sources on which the model is trained, and β_p are the coefficients of the model.

The predictors were chosen as a compromise between model simplicity and capturing the most important processes governing the ten unprecedented heatwaves analysed: Z500 is the most obvious choice given the importance of anticyclones for mid-latitude heatwaves. Because our model is based on region-average anomalies, the Z500 anomaly does not contain any information on the position of the anticyclone relative to WE, for which we include U500 and V500 as predictors. In addition, SM is included to capture the important role of low soil moisture during heatwaves. Finally, SSR is included to account for the diabatic contribution of radiation. This model is meant to be a simplified representation of the relevant physical processes that drive month-long temperature extremes in Western Europe. Inherently, it cannot capture processes involving variables not included in the model, or non-linear relationships, including, but not limited to, land-atmosphere feedbacks between soil moisture and temperature.

3 Results

The ten unprecedented heatwaves in our boosting simulations (U1–U10) exceed the most extreme historical heatwaves (H1–H10), not only in terms of absolute temperatures, but also when compared to their respective background climate. The anomalies of the unprecedented heatwaves range from $3.7\,\sigma$ (U10) to $4.3\,\sigma$ (U1), compared with $3.6\,\sigma$ for the most extreme historical heatwave in June/July 1976, the only historical heatwave to exceed an anomaly of $3\,\sigma$ (Figs. 1a, Tabs. A2 and A1). This is also

https://doi.org/10.5194/egusphere-2026-2005
Preprint. Discussion started: 28 April 2026

reflected in the return periods of these unprecedented heatwaves, with best estimates between around 600 years for U10 and 6000 years for U1. The 95 % confidence intervals of these estimates have lower bounds of roughly 400–2000 years and upper bounds of roughly 1500 years–∞, with infinite upper bounds for U1–U3 (Fig. 1b); see Sect. 2.4 for details on the calculation of return periods. Given that the central return period estimates for these unprecedented heatwaves are finite but much longer than a human lifetime, they appear statistically possible but (by definition) not probable.

In the following, we address the less straight-forward question of whether these heatwaves are plausible by assessing their physical conformity, internal consistency, and historical precedent. In practice, our assessments of these characterisations naturally overlap, but generally fall into two categories: By comparing the unprecedented heatwaves from CESM2 ensemble boosting simulations to less extreme heatwaves in the CESM2-LE, we assess whether they are internally consistent; by comparing them to historical heatwaves, we assess whether — despite their by definition unprecedented magnitude — these heatwaves are externally consistent with historical precedents. The conformity to physical principles represents the foundation of most of our assessment procedure; we test it by comparing the underlying physical processes in these unprecedented heatwaves both internally (within CESM2) and externally (with respect to ERA5).

3.1 Historical analogues

As a first test of plausibility, we search for multivariate historical analogues for the unprecedented heatwaves. For each unprecedented heatwave, we calculate the Euclidean distance between the anomalies of 30-day mean horizontal fields over Europe (12°W – 42°E, 35°N – 72°N) between the respective unprecedented heatwave and ERA5 (1965–2009), respectively. The best multivariate analogue for each unprecedented heatwave (listed in Tab. A3) is defined as the historical 30-day period that minimises the sum over the Euclidean distances of all 13 variables (TM, TX, TN, Z500, U500, V500, ω500, SSR, PREC, SM, LHF, SHF, and EF; see Tab. 1). In the following, we present two contrasting examples of multivariate analogues for unprecedented heatwaves that highlight both the power and limitations of this approach.

The first example is the most extreme heatwave in our simulations (U1), whose best multivariate analogue is the historical heatwave in June/July 1976 (Fig. 2). Note that while this multivariate analogue overlaps with the most extreme historical 30-day TM anomaly (H1), the two periods are shifted by approximately two weeks (Tabs. A2 and A3). Both U1 and its analogue feature very similar geographic distributions of TM anomalies, with particularly extreme anomalies over Great Britain and Northern France. Although in WE, the best analogue is still about 1σ less extreme than U1, it is among the most extreme historical heatwaves and exhibits many similarities to U1. The Z500 anomaly, although weaker and smaller, is located in a very similar region, as are the anomalies in U500 and V500, which are quite similar in magnitude in the vicinity of WE. Both U1 and its analogue feature relatively weak anomalies in ω500 and PREC over WE and similar distributions over most of Europe. For SSR, while the anomalies differ in WE, the overall spatial pattern still looks remarkably similar. The largest discrepancies are found in SM, SHF, and EF, where the 1976 analogue features much more extreme anomalies and thus appears to be much more diabatically driven than U1. This stronger diabatic contribution appears to be partly pre-conditioned: The precipitation anomalies in the months preceding the 1976 analogue are substantially lower than in the months preceding the U1 heatwave

https://doi.org/10.5194/egusphere-2026-2005
Preprint. Discussion started: 28 April 2026

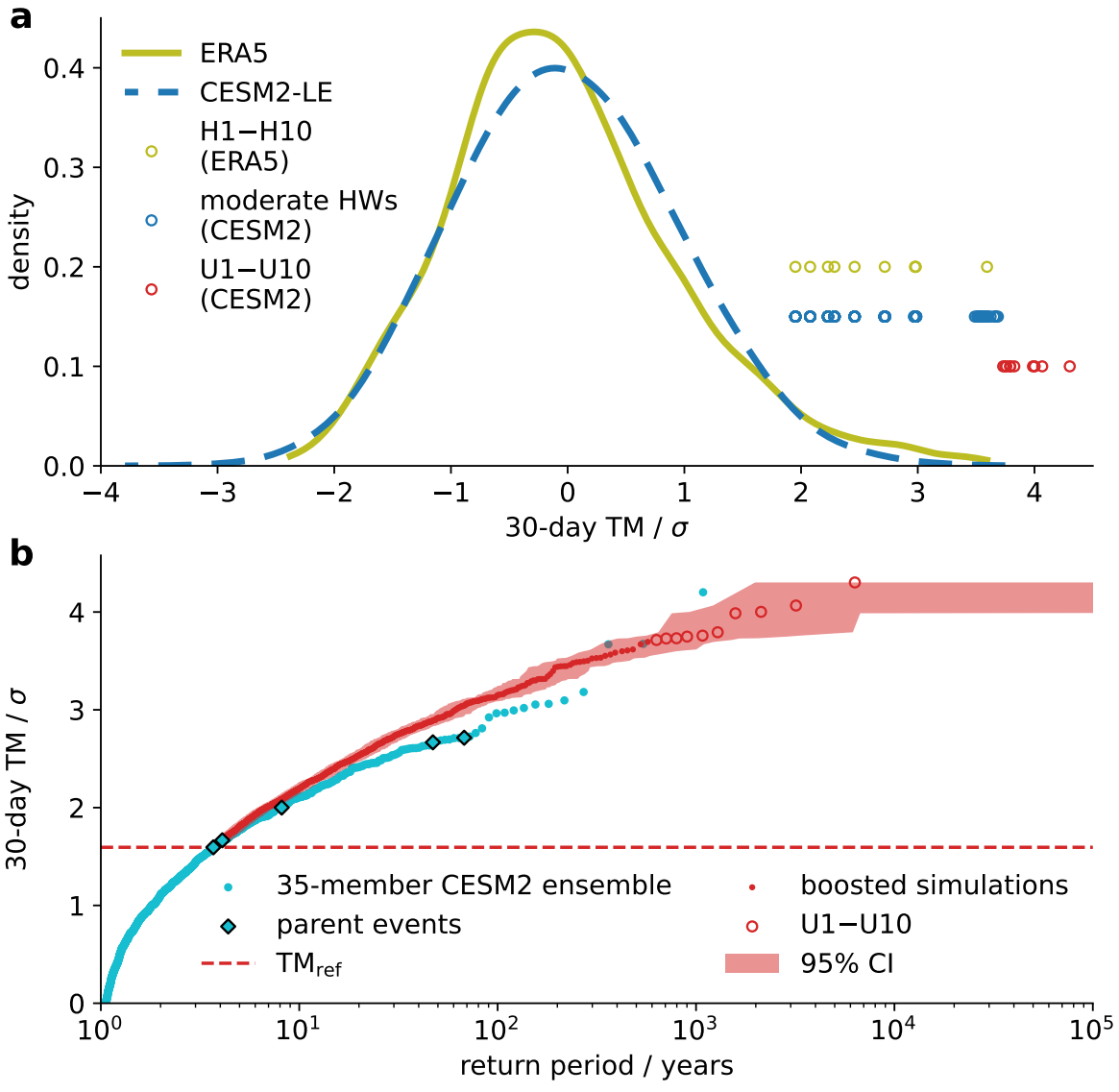

Figure 1. Contextualisation of selected unprecedented month-long heatwaves in Western Europe. (a) 30-day TM anomalies of the ten most extreme historical heatwaves in WE (H1–H10, yellow circles), 200 moderate extremes in the CESM2-LE with the same TM anomaly (blue circles), and the ten unprecedented heatwaves from ensemble boosting (U1–U10, red circles). They are compared to kernel density estimates of 30-day TM anomalies during the summer season (JJA) in ERA5 (1965–2009, yellow line) and the CESM2-LE (2005–2035, blue dashed line), using a Gaussian kernel with a bandwidth of 0.2 σ, truncated at the data limits. (b) Return period estimates of 30-day TM anomalies from boosting simulations (red dots), including U1–U10 (red circles), and their 95 % confidence interval (CI), as well as return period estimates of heatwaves in 35-member CESM2 ensemble (cyan dots), including the selected parent events (cyan diamonds).

https://doi.org/10.5194/egusphere-2026-2005
Preprint. Discussion started: 28 April 2026

(Fig. A2). This indicates that U1 could have been even more extreme if it had occurred on top of a similarly severe drought as the one that occurred in 1976.

The second example is the U4 heatwave, the most extreme unprecedented heatwave found outside the ensemble of the P1 parent heatwave. The best multivariate analogue we find for this heatwave is the historical heatwave of July 2006, which largely overlaps with H6, but is shifted by four days (Fig. 3, Tabs. A2 and A3). Compared to most of the other unprecedented heatwaves analysed, its most extreme TM anomalies are located further east over the Benelux region and North-Western Germany. In WE, the 2006 analogue is almost $2\,\sigma$ weaker than U4, and substantial discrepancies exist for many other variables as well: While the magnitude of the anticyclone is similar to U4, it is shifted to the South-East in the 2006 analogue, along with the anomaly in U500. U4 has a very pronounced spatial pattern in ω500, with sinking motion over the North and Baltic seas, near-zero vertical motion over WE, and rising motion over Northern Africa and the Western Mediterranean. This rising motion coincides with positive anomalies in V500, PREC, and SM and negative anomalies in SSR which exhibit characteristics of warm conveyor belts (Eckhardt et al., 2004) and atmospheric deserts, air masses originating from hot and dry boundary layers (Fix-Hewitt et al., 2026). In contrast, the 2006 analogue does not exhibit any of these features but instead features substantial subsidence over WE. Finally, the 2006 analogue does not capture the substantial anomalies in SM and EF during U4, highlighting yet another reason why the TM anomalies of these two heatwaves differ so substantially.

In conclusion, we find a remarkably similar multivariate historical analogue for the U1 heatwave centred over Great Britain and France, supporting the plausibility of this unprecedented heatwave. In contrast, we only find a much weaker and less similar historical analogue for the U4 heatwave centred over the Benelux region and Germany. Given that the existence of a similar historical analogue is not a necessary condition for plausibility, this does not imply that U4 is implausible; rather, it is consistent with the finding that Central Europe might have been lucky to not experience a more extreme heatwave so far (Thompson et al., 2023). Part of this limitation of the historical analogue method might be overcome by choosing a longer reanalysis data set, such as the Twentieth Century Reanalysis (Compo et al., 2011). However, by their very nature, unprecedented heatwaves often do not have comparable precedents in the observational record, but might still be plausible to occur in the future. In the following sections, we therefore perform more systematic and quantitative analyses that compare the simulated unprecedented heatwaves to a larger set of historical and simulated heatwaves of less extreme magnitudes.

3.2 Monthly anomalies in heatwave drivers

Next, we analyse the anomalies in different physical variables during the unprecedented heatwaves and compare them with the most extreme historical heatwaves (Fig. 4). For this, we first focus on the 30-day anomalies of these variables averaged over WE. As expected, all unprecedented heatwaves have positive anomalies in Z500, ranging from about $1.5\,\sigma$ to $3.0\,\sigma$. Most of these Z500 anomalies, including the most extreme U1 heatwave, are comparable in magnitude to the historical heatwave with the highest Z500 anomaly (H7, $2.6\,\sigma$). The anticyclones causing these positive Z500 anomalies also strongly disturb the zonal flow, which is seen by negative U500 anomalies in all unprecedented heatwaves. These anomalies are also mostly similar in magnitude to the most extreme historical heatwave (H6, -1.7σ) with the notable exception of U1, which reaches $-2.5\,\sigma$. In

https://doi.org/10.5194/egusphere-2026-2005
Preprint. Discussion started: 28 April 2026

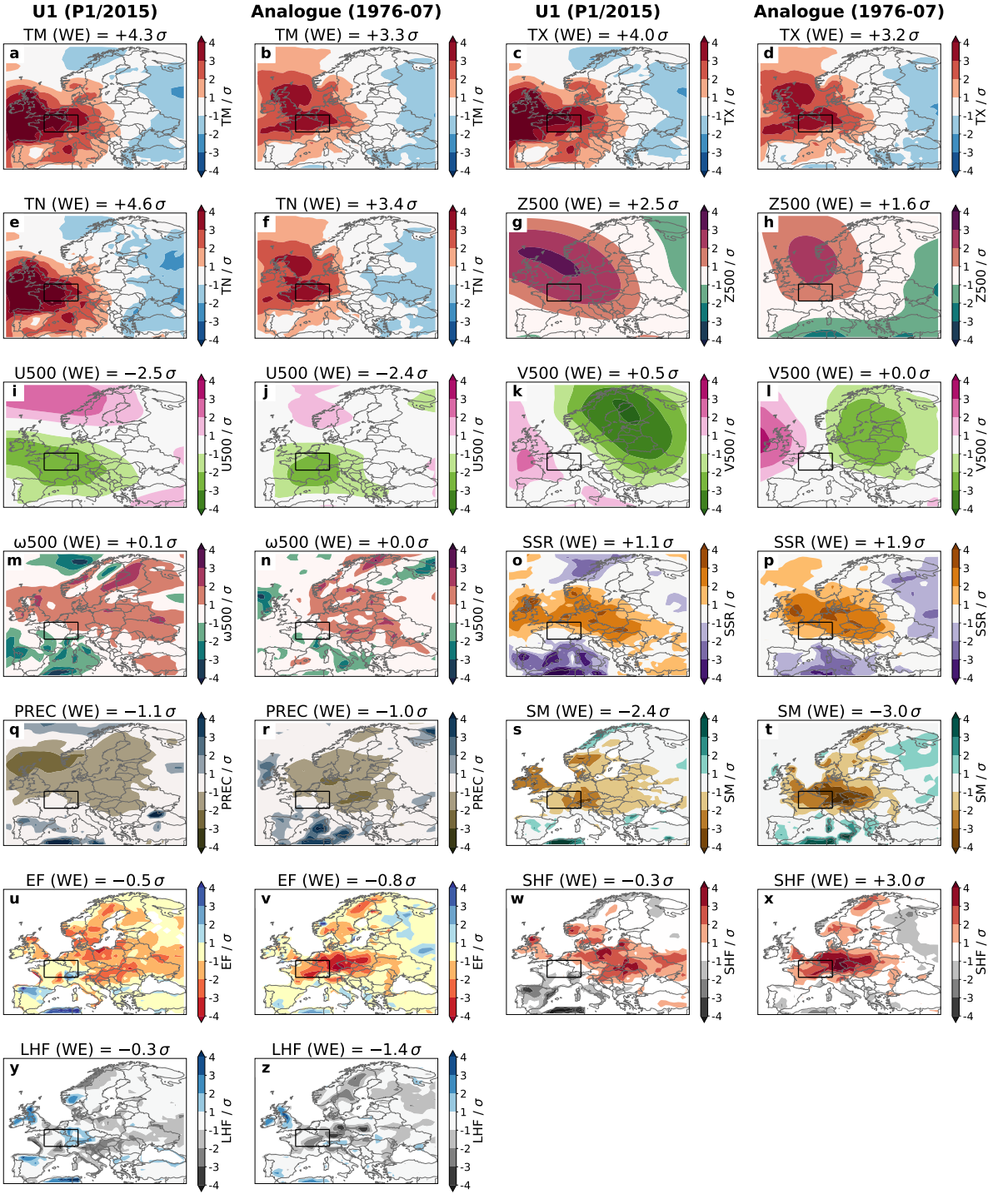

Figure 2. Horizontal fields in Europe of analysed variables during U1 heatwave (first and third columns) compared with the best historical analogue in July 1976 (second and fourth columns). The surface variables SM, EF, SHF, and LHF are only plotted over land.

https://doi.org/10.5194/egusphere-2026-2005
Preprint. Discussion started: 28 April 2026

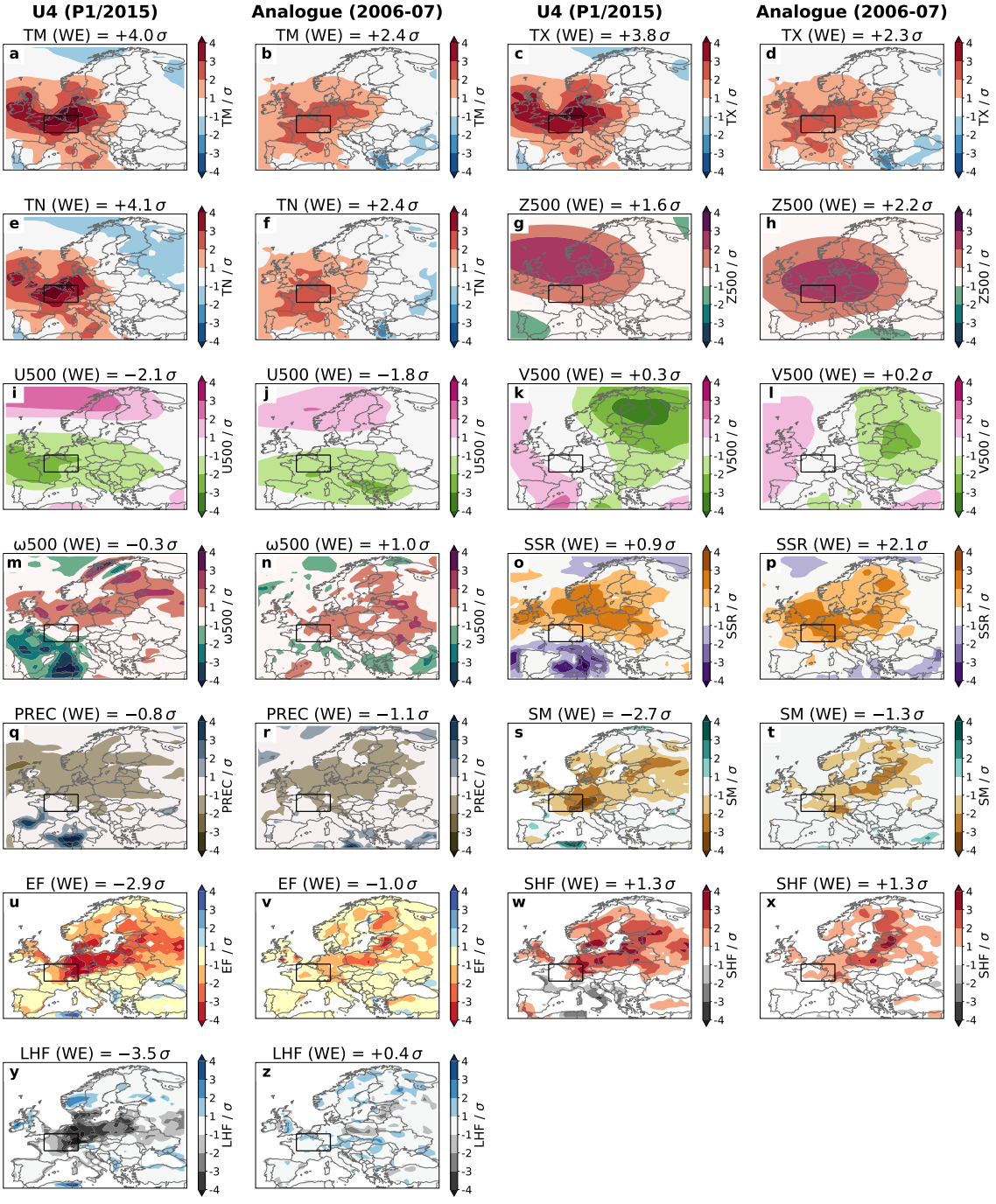

Figure 3. Horizontal fields in Europe of analysed variables during U4 heatwave (first and third columns) compared with the best historical analogue in July 2006 (second and fourth columns). The surface variables SM, EF, SHF, and LHF are only plotted over land.

https://doi.org/10.5194/egusphere-2026-2005
Preprint. Discussion started: 28 April 2026

contrast, the anomalies in SSR tend to be weaker in the unprecedented heatwaves compared to the historical heatwaves, in particular when comparing the five most extreme heatwaves, respectively.

The SM anomalies during the unprecedented heatwaves are much more negative than those of most historical heatwaves. However, the H2 and H1 heatwaves match and even exceed the magnitude of these negative simulated SM anomalies, respectively. This applies similarly to anomalies in EF, where only U8 slightly exceeds the negative anomaly of EF during H1. During historical heatwaves, large negative EF anomalies (H1 & H2) are mainly caused by large positive anomalies in SHF with negligible LHF anomalies; during unprecedented heatwaves with large negative EF anomalies (U4 & U8), the negative LHF anomalies are substantially larger in magnitude than the positive SHF anomalies. A possible explanation for this discrepancy is related to the projected long-term decrease in SM in Western Europe. Despite similar anomalies in SM, the absolute values of SM are around 15–20 % lower in U4 and U8 (model year 2031) than in the other unprecedented events (model year 2015). As a consequence, the same SM anomaly can imply that land-atmosphere fluxes are energy-limited during historical heatwaves, but moisture-limited (or transitional) in future heatwaves (Seneviratne et al., 2010). This is also consistent with the fact that historical heatwaves with less extreme SM anomalies tend to feature substantial positive LHF anomalies.

Other potential atmospheric drivers appear to play only a minor role during most of the analysed heatwaves. For V500, which we use as a proxy for mid-tropospheric temperature advection, only two unprecedented heatwaves (U8 & U9) and one historical heatwave (H5) have anomalies greater than $+1\,\sigma$. Similarly, for ω500, which we use as a proxy for adiabatic warming, only one simulated heatwave (U3) and one historical heatwave (H1) have anomalies greater than $+1\,\sigma$. This relatively minor role for advective and adiabatic processes might be affected by our simplified methodology. To disentangle and quantify the effects of different processes on air masses, Lagrangian approaches, for example based on back-trajectories, deliver more detailed results (Röthlisberger et al., 2025). Furthermore, the averaging period of 30 days can obscure more short-term anomalies in these drivers (see discussion in Sect. 3.3). Nevertheless, our analysis demonstrates that the simulated unprecedented heatwaves behave quite similarly to historical heatwaves when analysed from a Eulerian perspective.

To analyse the differences in physical drivers more systematically, we compare the distributions of their anomalies during historical and unprecedented heatwaves, as well as during moderate heatwaves in the CESM2-LE that have the same TM anomalies as the historical heatwaves (see Sect. 2.3 for details). We find that when comparing heatwaves of the same magnitudes (historical and moderate CESM2 heatwaves), most physical drivers feature very similar anomalies. The moderate CESM2 heatwaves tend to have slightly less positive anomalies in Z500, SSR, SHF, and LHF and slightly more negative SM anomalies, but only the difference in SSR exceeds $0.5\,\sigma$. This suggests that CESM2 can accurately capture the physical drivers present during heatwaves in ERA5 when comparing heatwaves of similar magnitude. Compared to moderate CESM2 heatwaves, the unprecedented heatwaves have more positive Z500 and SHF anomalies, and substantially more negative U500, SM, LHF and EF anomalies, while the median anomalies in SSR, ω500, V500 and PREC are virtually identical. The only physical driver whose sign of the median anomaly changes is LHF, consistent with the hypothesis outlined above. This suggests that unprecedented heatwaves in CESM2 are produced by "extreme anomalies of common drivers" (Fischer et al., 2021).

In conclusion, although the temperature anomalies during the simulated unprecedented heatwaves are, by definition, unprecedented, the anomalies of most analysed physical drivers have precedents in the historical record. However, compared to

https://doi.org/10.5194/egusphere-2026-2005
Preprint. Discussion started: 28 April 2026

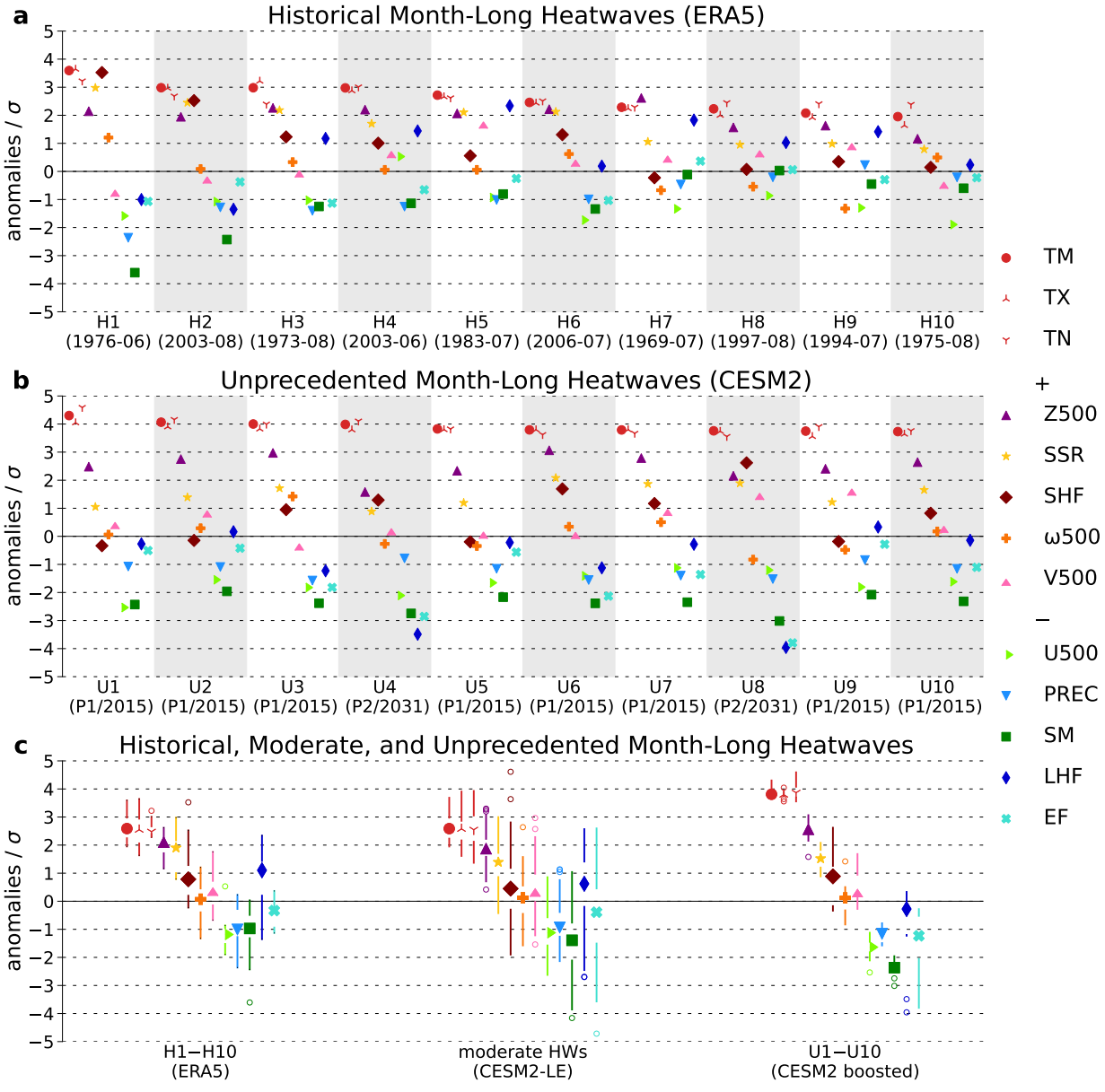

Figure 4. Anomalies of heatwave characteristics and drivers in WE (see Tab. 1). (a) Ten most extreme historical month-long heatwaves in ERA5 (H1–H10). (b) Ten most extreme unprecedented month-long heatwaves in CESM2 ensemble boosting simulations (U1–U10). (c) Box plots of anomalies in heatwave variables during historical heatwaves (H1–H10), moderate heatwaves (HWs), and unprecedented heatwaves (U1–U10): Median (filled symbols), inter-quartile range IQR (empty space), whiskers (1.5 IQR, solid lines) and outliers (empty circles). Shown are the temperature variables (red), and variables with expected positive ("+") and negative ("–") anomalies during heatwaves. This separation is a simplification primarily adopted for ease of visualization; several variables feature substantial anomalies of both signs during heatwaves.

https://doi.org/10.5194/egusphere-2026-2005
Preprint. Discussion started: 28 April 2026

any single historical heatwave, each unprecedented heatwave exceeds the anomaly in at least one analysed driver. Furthermore, most drivers show larger median anomalies in the unprecedented heatwaves compared to more moderate heatwaves in the CESM2-LE. We therefore preliminarily conclude that the combination of simultaneously extreme anomalies in several drivers, rather than an extreme anomaly in a single driver, appears to be responsible for the magnitude of most of these unprecedented heatwaves.

3.3 Temporal substructure

As a next step, we analyse the temporal substructure of the analysed heatwaves in terms of their daily anomalies. For historical, moderate, and unprecedented heatwaves, we rank the daily anomalies of the variables analysed above from highest to lowest within the respective 30-day period (Fig. 5), similar to the approach of Röthlisberger et al. (2020). Similarly to the 30-day anomalies analysed in the preceding section, the temporal substructure of these variables is very similar in the historical and moderate CESM2 heatwaves, with less positive anomalies in SSR, SHF, and LHF and more negative SM anomalies during the moderate heatwaves.

Unsurprisingly, the unprecedented heatwaves feature substantially larger daily TM anomalies throughout the 30-day period; this difference is greatest for the most extreme 15–20 days, a feature that is even more pronounced for TN, but slightly less pronounced for TX. The largest differences in physical drivers between the historical and the unprecedented heatwaves can be found in variables related to land-atmosphere exchanges. Compared with historical heatwaves, the unprecedented heatwaves have substantially weaker PREC on days with the highest PREC (ranked days 1–10), indicating more persistent meteorological droughts. A similar picture can be observed for SM, which is generally much lower in the unprecedented heatwaves, but particularly for the days with higher (less extreme) SM, indicating more persistent agricultural droughts. This also leads to unprecedented negative anomalies in LHF, whereas the ranked anomalies of PREC, SM, and EF in the unprecedented heatwaves are matched or even exceeded by the historical H1 heatwave.

Most other physical drivers feature very similar temporal substructures during the unprecedented heatwaves and the historical heatwaves, particularly SHF, ω500, V500, but also to a lesser extent Z500, U500, and SSR. These temporal substructures also reveal that the small 30-day mean anomalies in V500 and ω500 are partially due to the long averaging period: Short-term periods of southerly wind or vertical sinking are largely cancelled out by periods of negative anomalies as the anticyclone itself moves (Fig. 5g,h). For Z500 and U500, the unprecedented heatwaves exhibit a small and fairly uniform shift of the ranked anomalies towards more extreme values compared to historical heatwaves (more positive for Z500, more negative for U500). This indicates slightly stronger and slightly more persistent anticyclones that perturb the zonal flow more strongly throughout the 30-day periods. As already mentioned above, the unprecedented heatwaves exhibit less extreme SSR anomalies compared to historical heatwaves; as Fig. 5 shows, this is almost entirely limited to the 15 days with the most extreme SSR anomalies. At the same time, the ranked SSR anomalies in the unprecedented heatwaves are very similar to those during the moderate heatwaves from the CESM2-LE.

Another way of studying the temporal structure is to evaluate the persistence of different variables (see Sect. 2.5 for details). To this end, we compare the occurrence of periods in which the anomalies of TM and Z500 exceed $+1\,\sigma$, and in which the

https://doi.org/10.5194/egusphere-2026-2005
Preprint. Discussion started: 28 April 2026

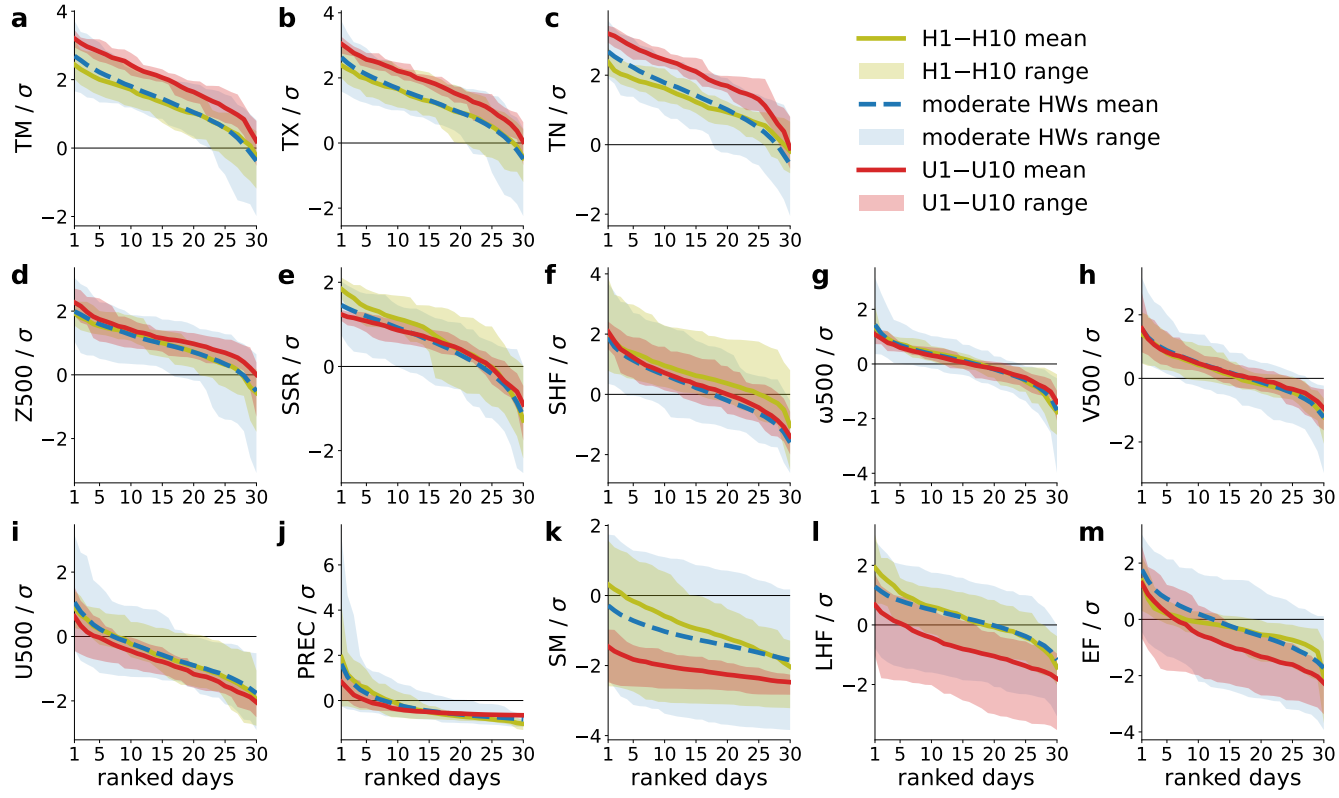

Figure 5. Ranked daily anomalies of heatwave characteristics and drivers during historical heatwaves (yellow), moderate heatwaves (blue), and unprecedented heatwaves (red). Shown are the temperature variables (a–c), and variables with generally positive (d–h) and generally negative (i–m) anomalies during heatwaves. Variables are sorted from highest to lowest anomalies, meaning that the most favourable conditions for heatwaves can be found at low ranked days panels (a)–(h), but at high ranked days for panels (i)–(m).

anomalies of U500 and SM remain below $-1\,\sigma$, respectively, between the unprecedented simulated heatwaves, ERA5, and the CESM2-LE (Fig. 6). With only one exception, the persistence in TM during the unprecedented heatwaves (red circles) is shorter than the historical record of 21 days (yellow line in Fig. 6a), and similar behaviour is found for both Z500 (Fig. 6b, two record-breaking events) and U500 (Fig. 6c, no record-breaking events). For both TM and Z500, CESM2 appears to capture the frequencies of short persistence periods ($<$10 days) quite well, but substantially underestimates the frequency of longer persistence periods, suggesting that these persistent events may be rarer in CESM2 than in the real world. This is consistent with the finding of previous studies that global circulation models (GCMs) struggle to reproduce persistent blocking regimes (Tibaldi and Molteni, 1990; Davini and D'Andrea, 2016; Liu et al., 2022). However, for persistence in U500, there does not appear to be a systematic bias in CESM2 relative to ERA5.

In contrast, CESM2 overestimates the frequency of long persistence periods in SM: The CESM2-LE simulates a much higher frequency of long persistence periods in SM ($>$15 days) and six unprecedented heatwaves feature persistence periods

https://doi.org/10.5194/egusphere-2026-2005
Preprint. Discussion started: 28 April 2026

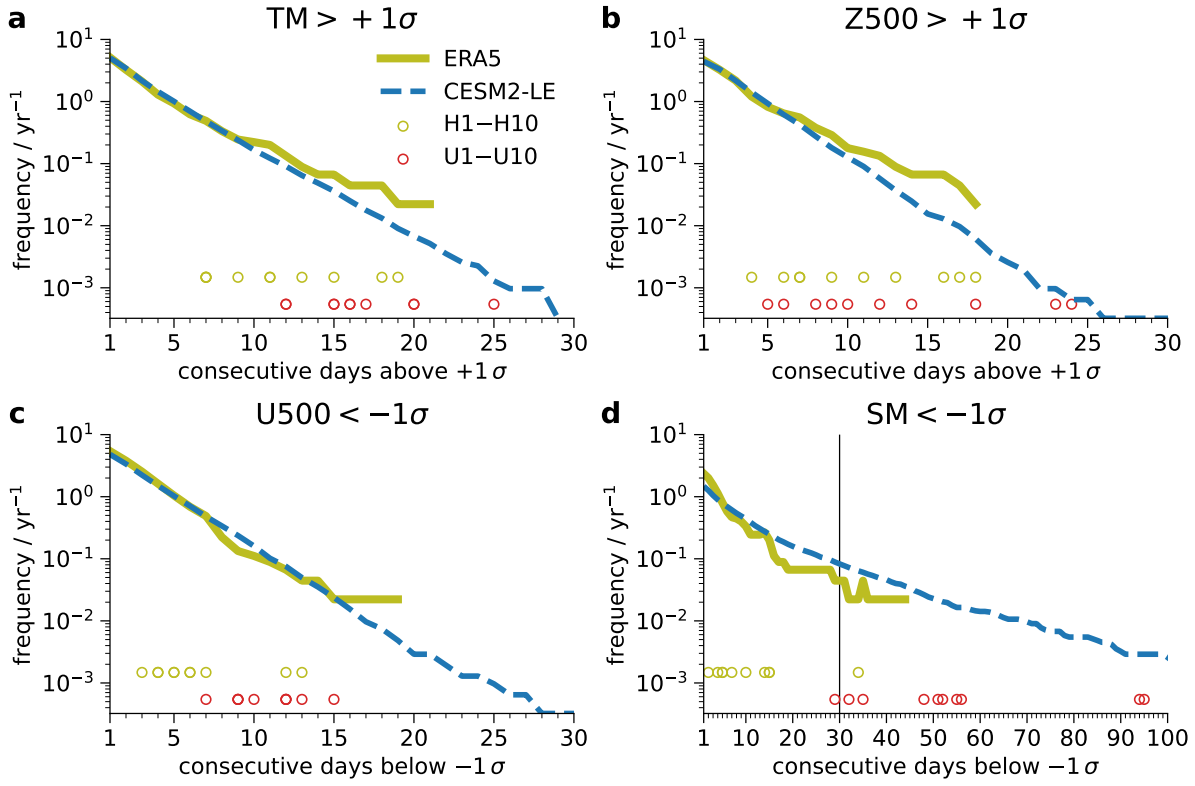

Figure 6. Persistence of TM, Z500, U500, and SM. Number of consecutive days in the summer season (JJA) where the daily anomaly is higher than $+1\sigma$ (for TM and Z500) or lower than -1σ (for U500 and SM), respectively. Shown are the relative frequencies in ERA5 (yellow) and the CESM2-LE (blue), compared to the values during the simulated unprecedented heatwaves U1–U10 (red circles) and the ten most extreme historical heatwaves H1–H10 (yellow circles). Note the different x-axis for SM in panel (d).

longer than the historical record (Fig. 6d). This is because, relative to ERA5-Land, CESM2 overestimates the occurrence of negative SM anomalies (Fig. A3). This is consistent with previous findings that (1) climate models tend to overestimate soil drying due to land-atmosphere feedbacks (Vogel et al., 2018) and (2) for heatwaves over land, CESM2 overestimates the diabatic contribution and underestimates the adiabatic contribution relative to ERA5 (Röthlisberger et al., 2025). In contrast, despite substantial regional and intermodel differences, monthly soil moisture memory is generally well represented in GCMs (Seneviratne et al., 2006). However, it should be noted that soil moisture is difficult to compare between CESM2 and ERA5 because reanalysis data sets also involve large uncertainties and should thus be interpreted with care.

In conclusion, the ranked anomalies during the simulated unprecedented heatwaves are largely in accordance with historical precedent, and the existing differences appear to be generally consistent between the different variables. In contrast, CESM2 struggles to accurately capture persistence periods relative to ERA5, in line with the existing literature. This means that the unprecedented heatwaves simulated by CESM2 occur for "partly the wrong reasons" (Röthlisberger et al., 2025). These biases

https://doi.org/10.5194/egusphere-2026-2005
Preprint. Discussion started: 28 April 2026

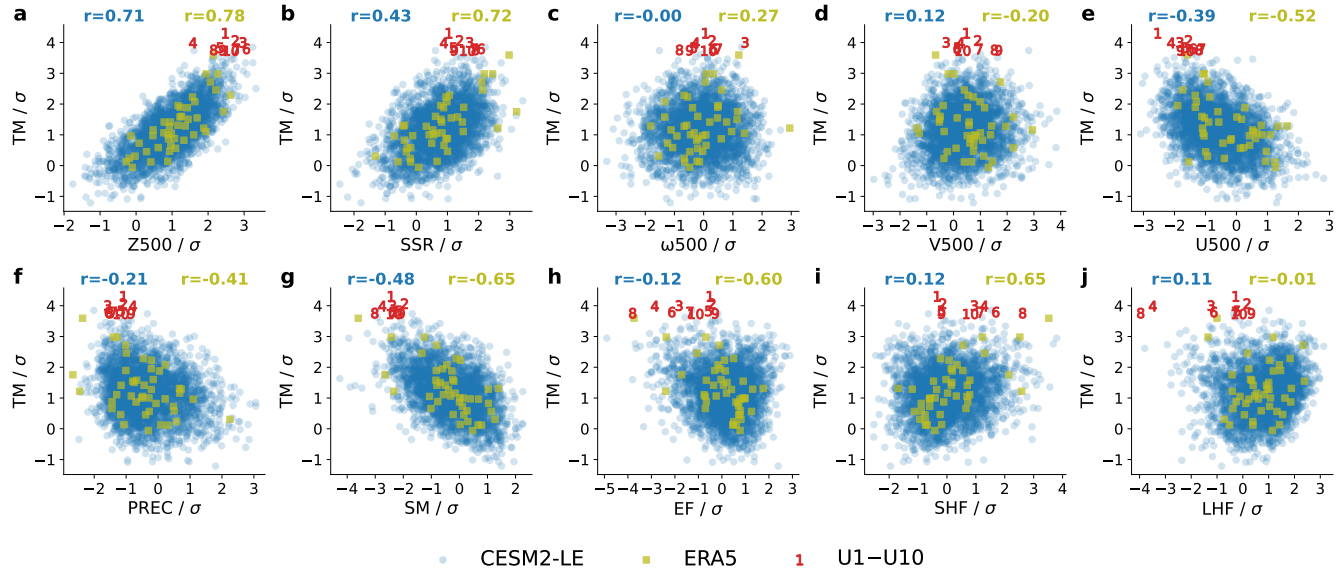

Figure 7. Bivariate distributions between TM and analysed heatwave drivers. Shown are the 30-day anomalies during the ten unprecedented heatwaves (red numbers) and during the maximum 30-day temperature anomaly in each summer season in both the CESM2-LE (2005–2035, blue circles) and ERA5 (1965–2009, yellow squares). For the CESM2-LE and ERA5 heatwaves, the correlation coefficient between the respective variables is noted at the top of the panel.

between the roles of diabatic and adiabatic contributions appear to partially compensate, but overall CESM2 still substantially underestimates the persistence in TM. The fact that the TM persistence periods during some unprecedented heatwaves nevertheless exceed the historical record suggests that heatwaves of comparable or even longer persistence are plausible to occur in the real world.

3.4 Bivariate relationships

Another way of assessing plausibility is to analyse bivariate relationships between different relevant physical variables. This serves to test in more detail whether the physical drivers during these unprecedented heatwaves conform to physical principles and whether anomalies in different drivers are internally consistent. For this, we select the maxima of the summer season (JJA) in 30-day z_{TM} in ERA5 (1965–2009, 45 heatwaves) and the CESM2-LE (2005–2035, 3100 heatwaves). We then compare the bivariate distributions of the 30-day anomalies in the drivers and characteristics of the unprecedented heatwaves with those of the heatwaves in ERA5 and the CESM2-LE (Figs. 7 and 8). All ten unprecedented heatwaves are more extreme in terms of the TM anomaly than the most extreme heatwave in ERA5 and more extreme than almost all heatwaves in the CESM2-LE, placing them at the edge of all bivariate distributions involving TM. The different physical drivers can be broadly grouped into three different categories.

https://doi.org/10.5194/egusphere-2026-2005
Preprint. Discussion started: 28 April 2026

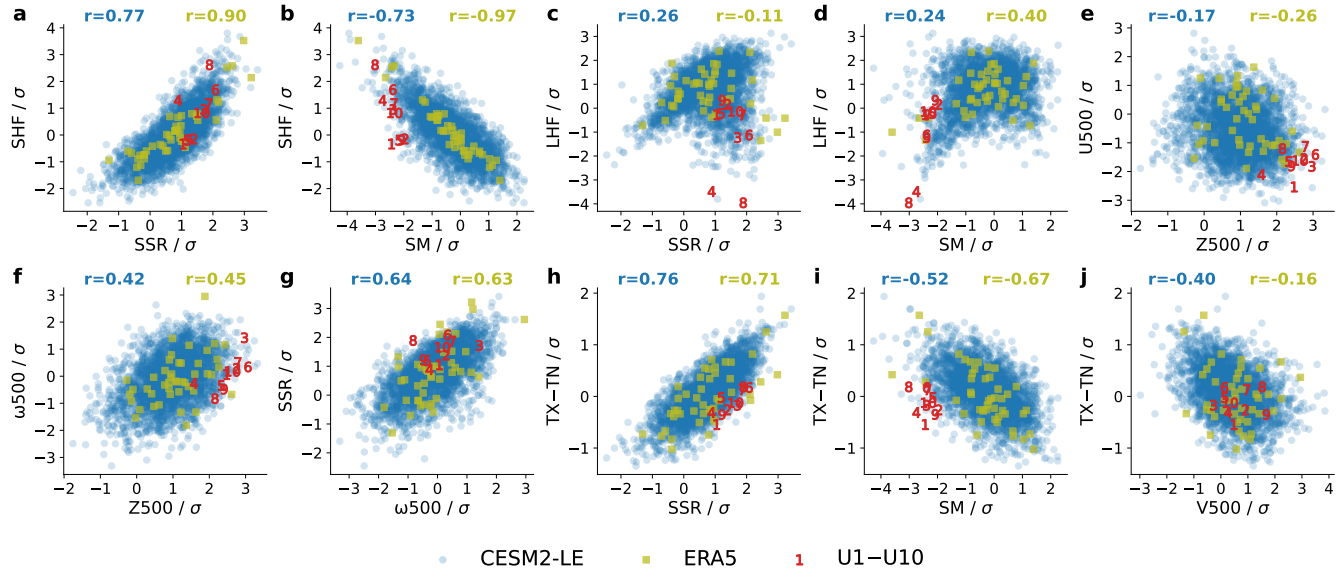

Figure 8. Same as Fig. 7, but for selected cross-relationships between different heatwave drivers and characteristics, including the diurnal temperature range (TX-TN), for which we subtract the anomalies in TN from those in TX.

First, several drivers exhibit comparatively strong correlations with TM, and their anomalies during the unprecedented heatwaves are also mostly at the extreme end relative to CESM2-LE and ERA5. This is the case for Z500 (Fig. 7a), U500 (Fig. 7e), SM (Fig. 7h) and, to a lesser extent, PREC (Fig. 7f). These correlations align with expectations from physical process understanding, highlighting the importance of blocking anticyclones and drought conditions that favour heatwaves. Furthermore, the anomalies of these drivers are consistent with other heatwaves in the CESM2-LE, but also with historical heatwaves in ERA5.

Second, ω500 (Fig. 7c) and V500 (Fig. 7d) have weak correlations with TM. For V500 this is not surprising given that temperature advection, by definition, mostly occurs non-locally. For ω500, this is in contradiction to the expectation that on average more extreme heatwaves would be associated with stronger sinking motion. This is presumably again because the 30-day mean can average out short periods of vertical sinking or southerly wind (see Sect. 3.3). Furthermore, as mentioned above, the Eulerian anomalies in WE on a single vertical level we use here do not capture the full effect of these processes; for example, the signal might be more pronounced on other vertical levels (Hotz et al., 2024). Nevertheless, the near-zero anomalies of many unprecedented heatwaves are quite similar to the behaviour of heatwaves in the CESM2-LE and ERA5, and the anomalies in ω500 appear to be consistent with the anomalies in Z500 (Fig. 8f) and in SSR (Fig. 8g).

Third, the relationships of surface heat flux variables with TM differ between CESM2 and ERA5. For EF and SHF in particular, CESM2 shows a much weaker correlation with T2M than ERA5 (Fig. 7h,i). This discrepancy should not be overinterpreted, given that ERA5 is notoriously not closing the (surface) energy budget (Hersbach et al., 2020). For LHF, both CESM2 and ERA5 show very weak correlations with T2M, but tend to show heteroscedastic behaviour: Average TM anomalies feature a

https://doi.org/10.5194/egusphere-2026-2005
Preprint. Discussion started: 28 April 2026

smaller spread in LHF than the most extreme TM anomalies, consistent with the fact that LHF anomalies vary strongly between the ten unprecedented heatwaves (Fig. 7j). This behaviour is not surprising given that surface fluxes strongly differ between moisture-limited and energy-limited conditions; during extreme conditions, this can be amplified through land-atmosphere feedbacks. When disentangling the behaviour of SHF and LHF with respect to SSR and SM, we find that SHF during the unprecedented heatwaves mostly follows the strongly linear relationships seen in ERA5 and the CESM2-LE (Figs. 8a,b). In contrast, LHF features strong non-linearities in both CESM2 and ERA5 (Figs. 8c,d). Most unprecedented heatwaves fall within the phase space covered by CESM2-LE and ERA5, whereas two heatwaves (U4 & U8) fall outside the range covered by ERA5 and are only similar to a single event in the CESM2-LE. This is again presumably due to their lower absolute values in SM, as described in Sect. 3.2.

The only variable that does not fall into any of these categories is SSR, which shows a generally solid positive linear correlation with TM (Fig. 7b). The SSR anomalies during the ten unprecedented heatwaves align with the most extreme heatwaves in the CESM2-LE; however, they are noticeably less extreme than expected from the bivariate distribution in ERA5. Nevertheless, the behaviours of other drivers appear to be mostly consistent with relatively weak SSR anomalies, most notably the anomalies in SHF (Fig. 8a) and ω500 (Fig. 8g). Furthermore, the diurnal temperature range (TX-TN) is also quite weak and is in line with the anomalies in SSR (Fig. 8h). Finally, the weak SSR anomaly is also presumably the reason why the diurnal temperature range is weaker than would be expected from the SM anomaly alone (Fig. 8i).

In conclusion, most of the bivariate relationships analysed are consistent with the bivariate distributions seen in heatwaves in both CESM2-LE and ERA5. In cases where this is not the case, this discrepancy appears to propagate to other variables in a physically consistent way. However, this still raises the question of how consistent the TM anomalies during the unprecedented heatwaves are given the combinations of anomalies in multiple different drivers.

3.5 Multivariate perspective

To address this question, we now analyse whether these heatwaves are consistent from a multivariate perspective. To this end, we employ a simple multilinear statistical model that infers the 30-day temperature anomaly based on the 30-day anomalies in a subset of five physical drivers: Z500, U500, V500, SM, and SSR. This selection is to some extent inherently arbitrary; it represents a compromise between model simplicity, predictor independence, and explained variance (see Sect. 2.6 for details).

We use six different versions of the multilinear model, separately trained to infer TM, TX, and TN based on heatwaves in the CESM2-LE and ERA5, respectively. These different versions of the model are then used to infer the 30-day anomalies in TM, TX, and TN, respectively, during the ten unprecedented heatwaves based on the anomalies in the five predictors (Fig. 9). The model trained on the CESM2-LE is primarily used to assess the internal consistency of unprecedented heatwaves. The model trained on ERA5 also evaluates these unprecedented heatwaves in terms of precedent, that is, whether the processes during these heatwaves are in line with those during observed historical heatwaves.

These models capture around 60–65 % of the variance in TN, around 75 % in TM, and around 80–85 % in TX. The lowest explained variance in TN is not surprising, because it is more strongly affected by processes not directly captured in our model, such as the downwelling longwave radiation from water vapour and clouds. Although our models explain the majority of the

https://doi.org/10.5194/egusphere-2026-2005
Preprint. Discussion started: 28 April 2026

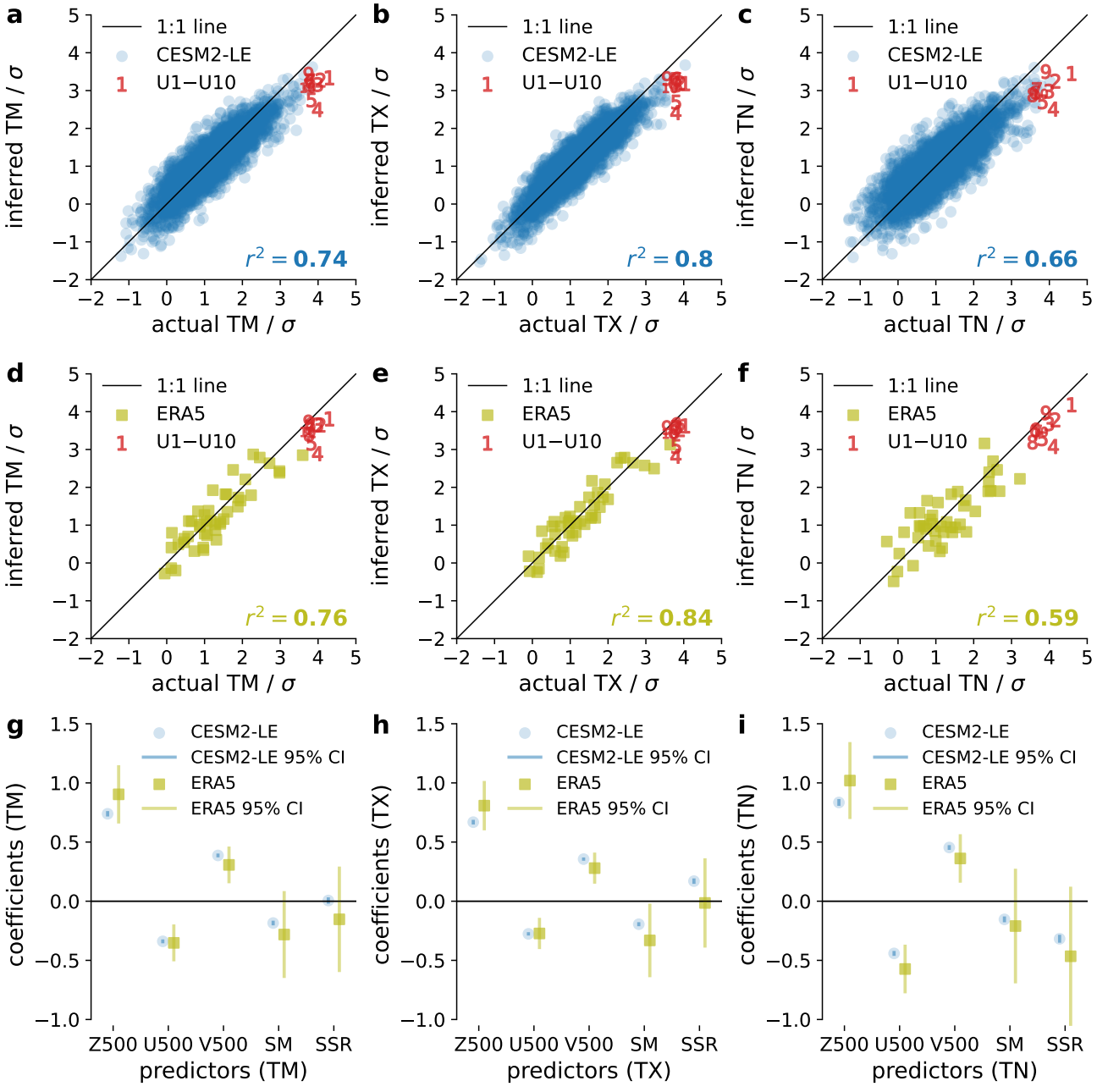

Figure 9. Actual anomalies of TM (a,d), TX (b,e), and TN (c,f) and anomalies inferred using our multilinear statistical model. Shown are the training data, namely the annual maxima of 30-day anomalies in WE during the summer season (JJA) in the CESM2-LE (a–c, blue circles) and in ERA5 (d–f, yellow squares), respectively. The model is applied to 30-day anomalies of TM, TX, and TN in WE during the unprecedented heatwaves U1–U10 (red numbers). For reference, the 1:1 line and the explained variance r^2 of each model are also shown. The regression coefficients of each predictor and their 95 % confidence intervals (CI) are compared for TM (g), TX (h), and TN (i).

https://doi.org/10.5194/egusphere-2026-2005
Preprint. Discussion started: 28 April 2026

variance in the training data and thus perform well on average, they tend to underestimate the magnitude of the most extreme heatwaves, both for the training data and for the unprecedented heatwaves to which it is applied. This is not surprising given that (1) models are trained to perform well in the most extreme heatwave in an average summer and are thus affected by regression to the mean, and (2) our simple least-squares approach neglects uncertainty in the independent variable and is thus sensitive to regression dilution (Pitkänen et al., 2016). This behaviour is further favoured by the strongly non-linear nature in particular of land-atmosphere interactions and our omission of several relevant variables to achieve model simplicity. However, the main goal here is not to perfectly capture all processes affecting TM anomalies, but rather to assess whether the ten unprecedented heatwaves behave similarly in a multivariate phase space compared to other simulated or observed heatwaves. In Fig. 9, this corresponds to the question whether the data points of the unprecedented heatwaves behave consistently with the most extreme heatwaves in the training data.

In general, most unprecedented heatwaves appear to behave similarly to heatwaves in both CESM2-LE and ERA5. In other words, although their magnitude is underestimated by our model, this underestimation is similar to the underestimation of the most extreme heatwaves in the training data. The magnitude of U5 and especially U4 is underestimated more strongly than comparable heatwaves in the training data; however, the magnitude of the deviation from the 1-1 line is still comparable to differences found for less extreme heatwaves in the training data. The underestimation of U4 is presumably enhanced by its lower absolute value of SM, as discussed in Sect. 3.2. Five of the six models include training data heatwaves of comparable magnitude to the unprecedented heatwaves, that is, the anomalies during U1–U10 only slightly exceed the most extreme heatwave in the training data. However, the TN anomalies of U1–U10 are far more extreme than any heatwave in ERA5 (Fig. 9f). Remarkably, despite this fact, the model trained on ERA5 only slightly underestimates the TN anomalies of the unprecedented heatwaves. This shows that these unprecedented heatwaves, despite their record-shattering magnitude, are governed by processes very similar to those of historical heatwaves.

Another way to assess plausibility from a multivariate perspective is through the model coefficients (Fig. 9g–i). In general, the differences in coefficients between the different prognostic variables exhibit physically reasonable behaviour. For example, the SSR coefficient is most positive for TX and most negative for TN, presumably due to the associated lower cloud cover during the night. These two effects appear to largely cancel, which is why the effect of SSR on TM is much smaller than that of the other variables analysed. Furthermore, SM seems to play a larger role for TX than for TN, presumably as a result of surface heat fluxes induced by solar heating during the day. In contrast, the coefficients of the adiabatic and advective variables (Z500, U500, V500) are much stronger for TN than for TX. The coefficients for the models trained on CESM2-LE and ERA5 are generally similar; they lie within their respective 95 % confidence intervals for all configurations. Compared to ERA5, CESM2 has less positive Z500 coefficients, more positive V500 coefficients, less negative SM coefficients, and systematically higher SSR coefficients (more positive for TX, less negative for TM and TN). However, these differences should be interpreted with care, given the large confidence intervals of the model coefficients trained on ERA5, caused by the small sample size and the high collinearity between SSR and SM in ERA5 (not shown).

In summary, all of our model versions can infer temperature anomalies during the unprecedented heatwaves with an accuracy comparable to that of the training data itself. Remarkably, this includes the model versions trained only on historical heatwaves

https://doi.org/10.5194/egusphere-2026-2005
Preprint. Discussion started: 28 April 2026

in ERA5. We can thus conclude that, although these unprecedented heatwaves are far more extreme than the most extreme historical heatwaves, they are externally consistent from a multivariate perspective.

4 Discussion & Limitations

We demonstrate the feasibility of our process-based plausibility assessment approach for heatwaves, since these represent the extreme events with the most solid understanding of the underlying physical processes. In principle, our approach can also be applied to other extreme events, but it should be noted that the physical drivers of these events are less well understood and in some cases less straight-forward to implement in our framework. For example, it should be quite straight-forward to apply our approach to large-scale events that can be realistically simulated in general circulation models, such as cold spells or droughts. For smaller-scale events, such as heavy convective precipitation or wind storms, high-resolution modelling may be required to test the plausibility of local processes in simulations.

Furthermore, there are a number of caveats and limitations of our approach that should be considered. First, while we often refer to the non-temperature variables analysed as heatwave "drivers", it is not always possible to cleanly separate cause and effect. For example, soil moisture can cause temperature anomalies, but can also be amplified by them through land-atmosphere feedbacks (Seneviratne et al., 2010). Therefore, one must be careful in asserting causality when interpreting anomalies in associated variables during heatwaves, especially at a monthly time scale. For this reason, we further analyse the partitioning of latent and sensible heat flux in the evaporative fraction and focus on internal consistency rather than causal relationships.

Another caveat already alluded to above concerns the use of V500, ω500, and SHF in WE as proxies for temperature advection, adiabatic sinking, and diabatic warming which neglects upstream and non-local processes. Furthermore, it is an oversimplification because it neglects the vertical variations of these variables throughout the atmosphere (Hotz et al., 2024). This can only be properly accounted for by taking a Lagrangian approach of calculating back-trajectories of air parcels within the heatwave region, as for example done by Röthlisberger et al. (2025). Our Eulerian approach has the advantage that it is much easier and less computationally expensive to implement and could therefore realistically be included in an operational assessment of plausibility (Kelder et al., 2022a). However, it should be noted that this Eulerian approach might be less appropriate when analysing other types of extreme events, such as heavy precipitation or wind storms, particularly at short time scales. In contrast, extremes on a monthly time scale might lend themselves more naturally to a Eulerian perspective due to the required persistence and stationarity of the associated weather systems.

As indicated earlier, finding historical analogues for heatwaves in a rapidly warming climate is inherently challenging, but is made possible by our approach of considering standardised anomalies relative to a time-evolving climatology (although the issue of small sample sizes in reanalysis remains). While useful, this view can in principle obscure the fact that the same anomaly might be plausible in past climates, but not necessarily in future climates. This is particularly true for non-negative variables that can exhibit substantial non-Gaussianity, such as PREC or SM, particularly when combined with a decreasing trend over time. But it can also complicate the interpretation of anomalies in U500, as it is not obvious whether negative U500 anomalies refer to weaker-than-average westerlies or rather easterly winds.

https://doi.org/10.5194/egusphere-2026-2005
Preprint. Discussion started: 28 April 2026

Furthermore, the time-evolving climatology itself is also subject to uncertainties. For example, the 30-year climatology is difficult to precisely constrain in regions where the last 20–30 years are unusually warm or cold due to internal variability. Nevertheless, it offers clear improvements in assessing the extremeness of an event relative to the climate in which it occurred compared to a climatology based on a fixed time period.

In addition to this, although standardised anomalies account for many model biases in both mean state and variability, some systematic differences between CESM2 and ERA5 are harder to remove. For example, compared to observations, GCMs tend to overestimate soil drying during heatwaves due to differences in the representation of land-atmosphere feedbacks (Vogel et al., 2018). The atmospheric circulation in GCMs is also known to be "too zonal", that is, they systematically underestimate the occurrence and persistence of atmospheric blocking — a major driver of heatwaves (Tibaldi and Molteni, 1990; Davini and D'Andrea, 2016; Liu et al., 2022). As shown in Sect. 3.3, these biases can partially compensate, leading to simulated heatwaves that occur for "partly the wrong reasons" (Röthlisberger et al., 2025). Despite these limitations, our analysis of the different underlying processes shows that simulated unprecedented heatwaves cannot be ruled out as implausible. Nevertheless, this does not mean that the simulated temperatures during these heatwaves should be taken at face value; rather, it is still important to perform a bias correction when, for example, studying the impact of a heatwave (Lüthi et al., 2024).

For simplicity, all unprecedented heatwaves analysed in this study are based on a single model (CESM2). However, given the well-documented intermodel differences among GCMs, it would be very valuable to repeat similar analyses with other models. In particular, models that have already been used to create climate storylines should be evaluated in this way, which could provide a better picture of how plausible extreme events they simulate are.

5 Conclusions

We present a process-based approach to assess the plausibility of unprecedented climate storylines. We apply it to month-long heatwaves in Western Europe that would exceed the most extreme historical heatwaves by around 5 K (Lüthi et al., 2024). Our approach uses standardised anomalies relative to a time-evolving climatology of various heatwave drivers and compares them between simulated unprecedented heatwaves and historical heatwaves. We compare the ten most extreme month-long heatwaves in Western Europe from CESM2 ensemble boosting simulations with the ten most extreme historical month-long heatwaves in ERA5 relative to the respective background climate.

The anomalies of most heatwave drivers are slightly more intense on average during the unprecedented heatwaves, but they are comparable in magnitude and very similar in temporal substructure to observed historical heatwaves. However, CESM2 underestimates the persistence in Z500, while it overestimates the persistence in SM, indicating that the long persistences of these unprecedented heatwaves occur for "partly the wrong reasons" (Röthlisberger et al., 2025). On the whole, CESM2 underestimates the frequency of long temperature persistence, indicating that even longer-lasting heatwaves could be plausible to occur in the real world. Finally, the unprecedented heatwaves are also consistent internally within CESM2 and externally compared to ERA5 when analysed from a multivariate perspective, indicating that they are caused by "extreme anomalies of common drivers" (Fischer et al., 2021). Overall, despite some discrepancies between the unprecedented heatwaves and

https://doi.org/10.5194/egusphere-2026-2005
Preprint. Discussion started: 28 April 2026

the historical heatwaves, our analysis shows that the drivers and characteristics of these heatwaves conform with physical principles, are internally consistent and align well with historical precedents. From this we conclude that these unprecedented heatwaves cannot be ruled out as implausible, and thus such events should be included in risk assessments when preparing adaptation measures.

The possible ways to assess the plausibility of extreme weather and climate events are as diverse as the exact definition of plausibility itself (van der Helm, 2006). With our approach presented here, we show a way to perform this assessment that builds on existing approaches (Vautard et al., 2019; Kelder et al., 2022b) and on our understanding of the relevant physical processes during heatwaves developed by the community over the years (Barriopedro et al., 2023). Although the exact methodology needs to be modified depending on the type of extreme event that is analysed, our approach contains many ingredients that can provide powerful insights into the plausibility of different extreme events. This includes the use of a time-evolving climatology to meaningfully compare anomalies across different background climates, as well as a multivariate perspective that provides a holistic picture of the underlying dynamics of unprecedented events.

Focusing on plausibility rather than probability of unprecedented events is useful in a wide range of fields, ranging from epidemiology to economics (Derbyshire, 2022; Goodwin and Wright, 2010). This is because studying extreme events that are considered plausible — irrespective of their probability of occurrence — allows for the exploration of future scenarios while embracing inherent uncertainties (Selin and Guimarães Pereira, 2013). Therefore, studying plausible future extremes is essential for providing tangible what-if scenarios that are needed to educate disaster preparation.

Code and data availability. The code used to perform the analysis in this manuscript is available at https://doi.org/10.5281/zenodo.19492890 (Roemer et al., 2026a). Pre-processed data to reproduce the figures in this manuscript is available at https://doi.org/10.5281/zenodo.19494786 (Roemer et al., 2026b). The CESM2-LE data are publicly available from the NSF NCAR Geoscience Data Exchange at https://gdex.ucar.edu/datasets/d651056/ (Danabasoglu et al., 2020; Rodgers et al., 2021). The reanalysis data is publicly available from the Copernicus Climate Change Service Climate Data Store: ERA5 data on pressure levels at https://doi.org/10.24381/cds.bd0915c6 (Hersbach et al., 2023a), ERA5 data on single levels at https://doi.org/10.24381/cds.adbb2d47 (Hersbach et al., 2023b), and ERA5-Land data at https://doi.org/10.24381/cds.e9c9c792 (Muñoz-Sabater, 2019).

Appendix A: Selected heatwaves

This appendix provides more detailed information (exact period and 30-day TM anomalies) on the ten unprecedented heatwaves (U1–U10, Tab. A1) and the ten historical heatwaves (H1–H10, Tab. A2) analysed in this manuscript. For the unprecedented heatwaves, further details are given on the selected ensemble members (Tab. A1), the historical analogues detected (Tab. A3), and the daily TM anomalies during the unprecedented heatwaves (Fig. A1). Furthermore, we provide additional details on the PREC anomalies preceding the unprecedented U1 heatwave and its historical analogue (Fig. A2), as well as on the climatological differences in SM between ERA5-Land and the CESM2-LE (Fig. A3).

https://doi.org/10.5194/egusphere-2026-2005
Preprint. Discussion started: 28 April 2026

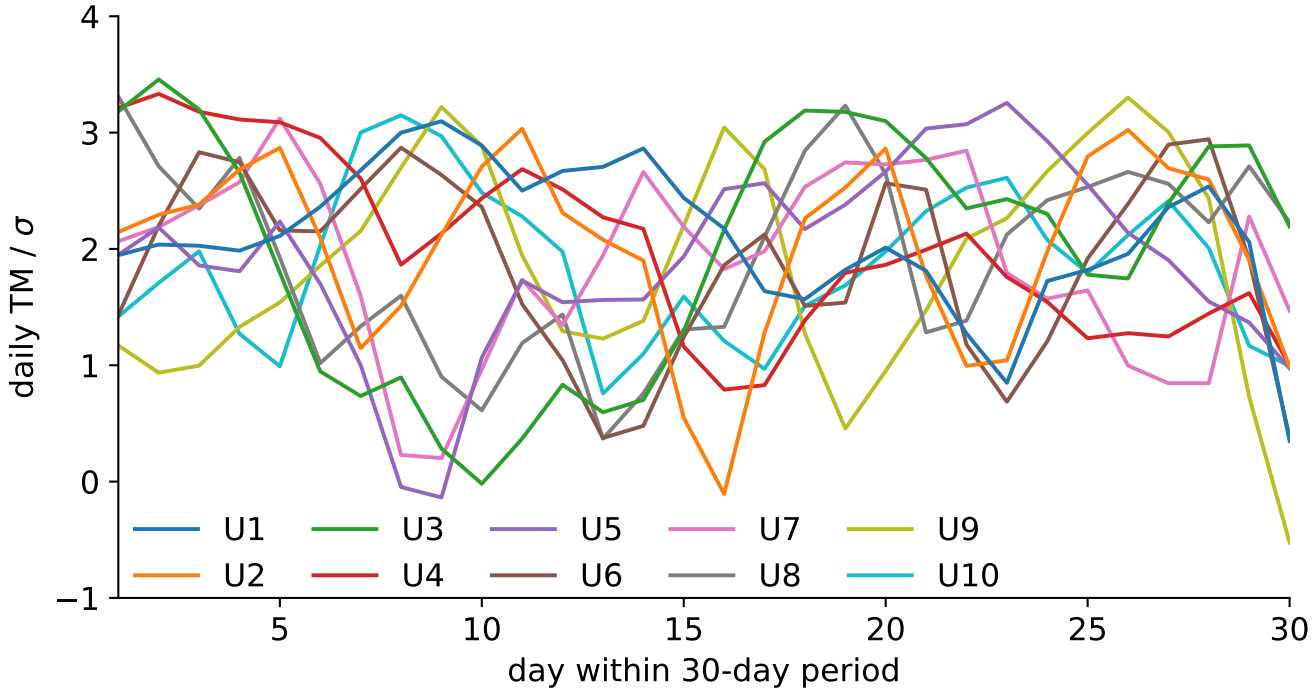

Figure A1. Daily TM anomalies during the ten selected unprecedented 30-day heatwaves (U1–U10).

Table A1. Ten unprecedented 30-day heatwaves in WE simulated using ensemble boosting in CESM2. Listed are the parent heatwaves, the date of re-initialisation, the selected ensemble member, the beginning and end of the selected 30-day period, and the 30-day TM anomaly during that period.

heatwave	parent	re-initialisation	member	day 1	day 30	TM / σ
U1	P1	2015-07-09	3	2015-07-25	2015-08-23	4.3
U2	P1	2015-07-11	37	2015-07-27	2015-08-25	4.1
U3	P1	2015-07-16	7	2015-07-30	2015-08-28	4.0
U4	P2	2031-07-12	29	2031-07-23	2031-08-21	4.0
U5	P1	2015-07-17	50	2015-07-26	2015-08-24	3.8
U6	P1	2015-07-12	62	2015-07-30	2015-08-28	3.8
U7	P1	2015-07-17	63	2015-07-23	2015-08-21	3.8
U8	P2	2031-07-13	76	2031-07-31	2031-08-29	3.8
U9	P1	2015-07-16	47	2015-07-22	2015-08-20	3.7
U10	P1	2015-07-13	6	2015-07-24	2015-08-22	3.7

Author contributions. FR, EF, and RK conceived the idea for this study. FR carried out the analysis and drafted the manuscript. EF and RN helped with developing and refining the methodology. All authors contributed to discussing the results and revising the manuscript.

https://doi.org/10.5194/egusphere-2026-2005
Preprint. Discussion started: 28 April 2026

Table A2. Ten historical 30-day heatwaves (HW) in WE selected from ERA5. Listed are the beginning and end of the selected 30-day period and the 30-day TM anomaly during that period.

heatwave	day 1	day 30	TM / σ
H1	1976-06-07	1976-07-06	3.6
H2	2003-08-01	2003-08-30	3.0
H3	1973-08-11	1973-08-09	3.0
H4	2003-05-29	2003-06-27	3.0
H5	1983-07-03	1983-08-01	2.7
H6	2006-07-01	2006-07-30	2.5
H7	1969-07-16	1969-08-15	2.3
H8	1997-08-08	1997-09-06	2.2
H9	1994-07-11	1994-08-09	2.1
H10	1975-07-30	1975-08-28	2.0

Table A3. Selected analogues from the ERA5 reanalysis for the ten unprecedented heatwaves simulated in CESM2 ensemble boosting simulations. Listed are the beginning and end of the selected 30-day period and the 30-day TM anomaly during that period

unprecedented heatwave	historical analogue day 1	historical analogue day 30	analogue TM / σ
U1	1976-06-21	1976-07-20	3.3
U2	2003-05-21	2003-06-23	2.6
U3	1973-08-11	1973-09-09	3.0
U4	2006-06-29	2006-07-28	2.4
U5	2006-07-01	2006-07-30	2.5
U6	1976-06-21	1976-07-20	3.3
U7	2003-07-19	2003-08-17	2.8
U8	2003-05-24	2003-06-22	2.5
U9	2003-05-24	2003-06-22	2.5
U10	2006-07-01	2006-07-30	2.5

Competing interests. At least one of the (co-)authors is a member of the editorial board of Weather and Climate Dynamics.

Acknowledgements. We thank U. Beyerle for technical assistance with the running and data acquisition of CESM2. We also thank L. Bloin-Wibe for help in calculating return periods, G. Gyuleva for useful input on the statistical model, A. Prein for help with acquiring additional CESM2 data, and P. Stott for encouraging feedback on an early version of this work. RN has received funding from the Swiss National Science Foundation (SNSF) through grant No. 216710. RK is part of SPEED2ZERO, a Joint Initiative co-financed by the ETH Board.

https://doi.org/10.5194/egusphere-2026-2005
Preprint. Discussion started: 28 April 2026

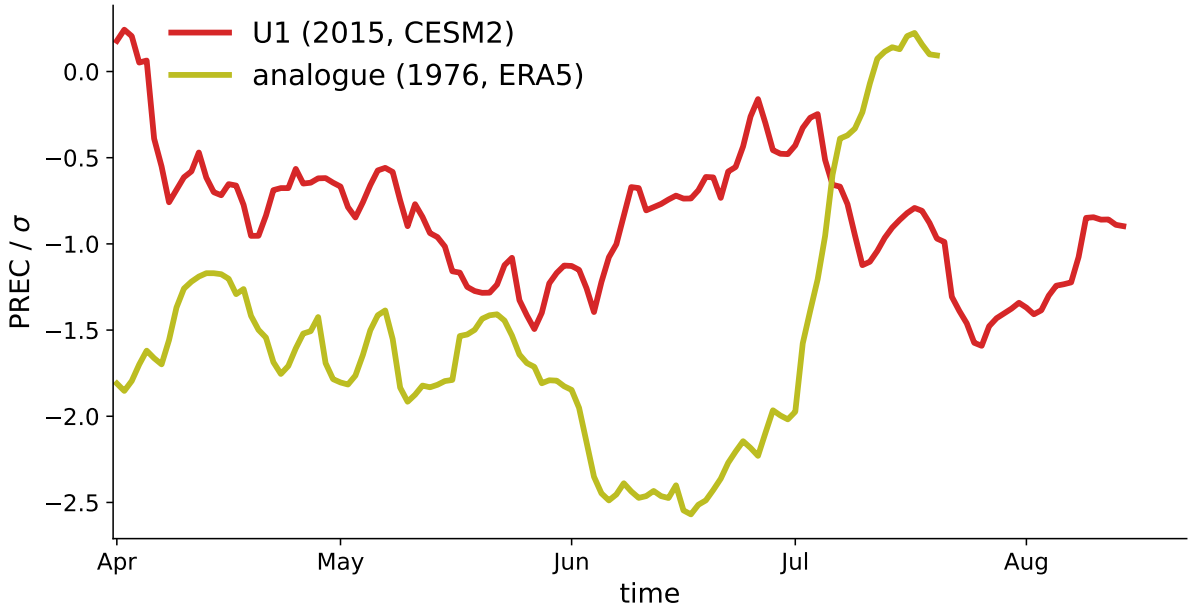

Figure A2. 30-day running mean PREC anomalies in the months preceding the U1 heatwave and its 1976 historical analogue.

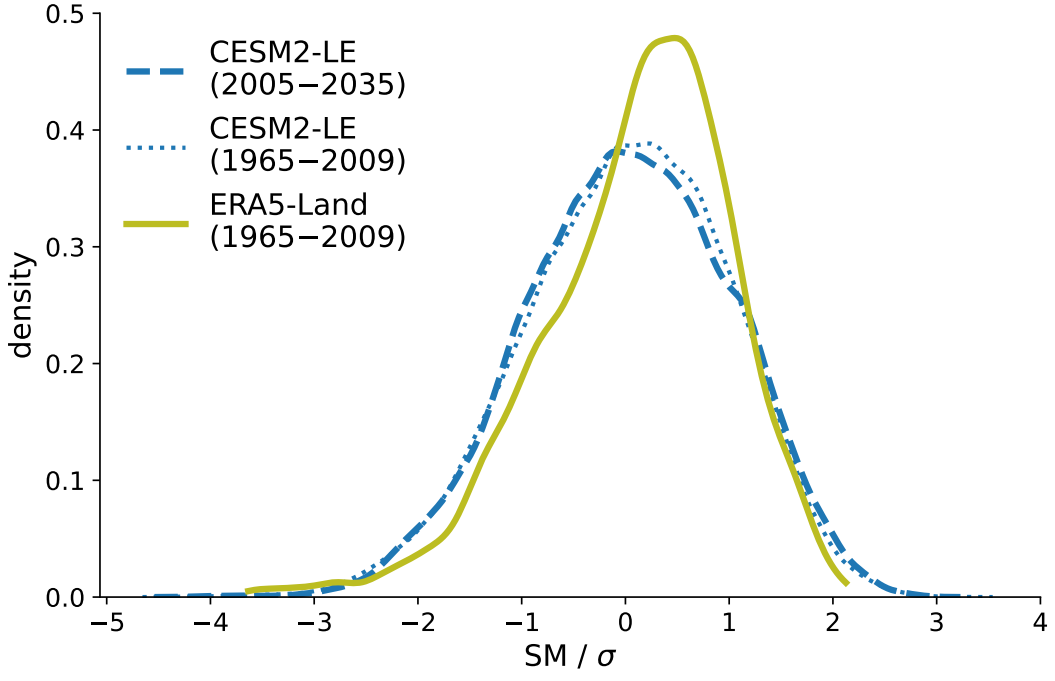

Figure A3. Kernel density estimates of 30-day SM anomalies during the summer season (JJA) in ERA5-Land (1965–2009, yellow) and in the CESM2-LE (1965–2009 and 2005–2035, blue).

https://doi.org/10.5194/egusphere-2026-2005
Preprint. Discussion started: 28 April 2026

References

Amara, R.: Views on futures research methodology, Futures, 23, 645–649, https://doi.org/10.1016/0016-3287(91)90085-G, 1991.

Anderson, G. B. and Bell, M. L.: Heat Waves in the United States: Mortality Risk during Heat Waves and Effect Modification by Heat Wave Characteristics in 43 U.S. Communities, Environmental Health Perspectives, 119, 210–218, https://doi.org/10.1289/ehp.1002313, 2011.

Bador, M., Terray, L., Boé, J., Somot, S., Alias, A., Gibelin, A.-L., and Dubuisson, B.: Future summer mega-heatwave and record-breaking temperatures in a warmer France climate, Environmental Research Letters, 12, 074 025, https://doi.org/10.1088/1748-9326/aa751c, 2017.

Baldissera Pacchetti, M., Coulter, L., Dessai, S., Shepherd, T. G., Sillmann, J., and Van Den Hurk, B.: Varieties of approaches to constructing physical climate storylines: A review, WIREs Climate Change, 15, e869, https://doi.org/10.1002/wcc.869, 2024.

Barriopedro, D., Fischer, E. M., Luterbacher, J., Trigo, R. M., and García-Herrera, R.: The Hot Summer of 2010: Redrawing the Temperature Record Map of Europe, Science, 332, 220–224, https://doi.org/10.1126/science.1201224, 2011.

Barriopedro, D., García-Herrera, R., Ordóñez, C., Miralles, D. G., and Salcedo-Sanz, S.: Heat Waves: Physical Understanding and Scientific Challenges, Reviews of Geophysics, 61, e2022RG000 780, https://doi.org/10.1029/2022RG000780, 2023.

Bartusek, S., Kornhuber, K., and Ting, M.: 2021 North American heatwave amplified by climate change-driven nonlinear interactions, Nature Climate Change, 12, 1143–1150, https://doi.org/10.1038/s41558-022-01520-4, 2022.

Baulenas, E., Versteeg, G., Terrado, M., Mindlin, J., and Bojovic, D.: Assembling the climate story: use of storyline approaches in climate-related science, Global Challenges, 7, 2200 183, https://doi.org/10.1002/gch2.202200183, 2023.

Black, E., Blackburn, M., Harrison, G., Hoskins, B., and Methven, J.: Factors contributing to the summer 2003 European heatwave, Weather, 59, 217–223, https://doi.org/10.1256/wea.74.04, 2004.

Bloin-Wibe, L., Noyelle, R., Humphrey, V., Beyerle, U., Knutti, R., and Fischer, E.: Estimating return periods for extreme events in climate models through Ensemble Boosting, Weather and Climate Dynamics, 6, 1147–1177, https://doi.org/10.5194/wcd-6-1147-2025, 2025.

Compo, G. P., Whitaker, J. S., Sardeshmukh, P. D., Matsui, N., Allan, R. J., Yin, X., Gleason, B. E., Vose, R. S., Rutledge, G., Bessemoulin, P., Brönnimann, S., Brunet, M., Crouthamel, R. I., Grant, A. N., Groisman, P. Y., Jones, P. D., Kruk, M. C., Kruger, A. C., Marshall, G. J., Maugeri, M., Mok, H. Y., Nordli, O., Ross, T. F., Trigo, R. M., Wang, X. L., Woodruff, S. D., and Worley, S. J.: The Twentieth Century Reanalysis Project, Quarterly Journal of the Royal Meteorological Society, 137, 1–28, https://doi.org/10.1002/qj.776, _eprint: https://rmets.onlinelibrary.wiley.com/doi/pdf/10.1002/qj.776, 2011.

Copernicus Climate Change Service: Heatwaves contribute to the warmest June on record in western Europe | Copernicus, https://climate.copernicus.eu/heatwaves-contribute-warmest-june-record-western-europe, 2025.

Danabasoglu, G., Deser, C., Rodgers, K., and Timmermann, A.: CESM2 Large Ensemble, https://doi.org/10.26024/kgmp-c556, 2020.

Davini, P. and D'Andrea, F.: Northern Hemisphere Atmospheric Blocking Representation in Global Climate Models: Twenty Years of Improvements?, Journal of Climate, 29, 8823–8840, https://doi.org/10.1175/JCLI-D-16-0242.1, 2016.

Derbyshire, J.: Increasing Preparedness for Extreme Events using Plausibility-Based Scenario Planning: Lessons from COVID-19, Risk Analysis, 42, 97–104, https://doi.org/10.1111/risa.13827, 2022.

D'Ippoliti, D., Michelozzi, P., Marino, C., de'Donato, F., Menne, B., Katsouyanni, K., Kirchmayer, U., Analitis, A., Medina-Ramón, M., Paldy, A., Atkinson, R., Kovats, S., Bisanti, L., Schneider, A., Lefranc, A., Iñiguez, C., and Perucci, C. A.: The impact of heat waves on mortality in 9 European cities: results from the EuroHEAT project, Environmental Health, 9, 37, https://doi.org/10.1186/1476-069X-9-37, 2010.

https://doi.org/10.5194/egusphere-2026-2005
Preprint. Discussion started: 28 April 2026

Dole, R., Hoerling, M., Perlwitz, J., Eischeid, J., Pegion, P., Zhang, T., Quan, X.-W., Xu, T., and Murray, D.: Was there a basis for anticipating the 2010 Russian heat wave?, Geophysical Research Letters, 38, https://doi.org/10.1029/2010GL046582, 2011.

Domeisen, D. I. V., Eltahir, E. A. B., Fischer, E. M., Knutti, R., Perkins-Kirkpatrick, S. E., Schär, C., Seneviratne, S. I., Weisheimer, A., and Wernli, H.: Prediction and projection of heatwaves, Nature Reviews Earth & Environment, 4, 36–50, https://doi.org/10.1038/s43017-022-00371-z, 2023.

Drouard, M. and Woollings, T.: Contrasting Mechanisms of Summer Blocking Over Western Eurasia, Geophysical Research Letters, 45, 12,040–12,048, https://doi.org/10.1029/2018GL079894, 2018.

Easterling, D. R., Meehl, G. A., Parmesan, C., Changnon, S. A., Karl, T. R., and Mearns, L. O.: Climate Extremes: Observations, Modeling, and Impacts, Science, 289, 2068–2074, https://doi.org/10.1126/science.289.5487.2068, 2000.

Eckhardt, S., Stohl, A., Wernli, H., James, P., Forster, C., and Spichtinger, N.: A 15-Year Climatology of Warm Conveyor Belts, Journal of Climate, 17, 218–237, https://doi.org/10.1175/1520-0442(2004)017<0218:AYCOWC>2.0.CO;2, 2004.

Feser, F., Van Garderen, L., and Hansen, F.: The Summer Heatwave 2022 over Western Europe: An Attribution to Anthropogenic Climate Change, Bulletin of the American Meteorological Society, 105, E2175–E2179, https://doi.org/10.1175/BAMS-D-24-0017.1, 2024.

Finkel, J. and O'Gorman, P. A.: Bringing Statistics to Storylines: Rare Event Sampling for Sudden, Transient Extreme Events, Journal of Advances in Modeling Earth Systems, 16, e2024MS004 264, https://doi.org/10.1029/2024MS004264, _eprint: https://agupubs.onlinelibrary.wiley.com/doi/pdf/10.1029/2024MS004264, 2024.

Finkel, J. and O'Gorman, P. A.: Rare Event Sampling for Moving Targets: Extremes of Temperature and Daily Precipitation in a General Circulation Model, Journal of Advances in Modeling Earth Systems, 18, e2025MS005 456, https://doi.org/10.1029/2025MS005456, _eprint: https://agupubs.onlinelibrary.wiley.com/doi/pdf/10.1029/2025MS005456, 2026.

Fischbacher-Smith, D.: Beyond the worst case scenario: 'Managing' the risks of extreme events, Risk Management, 12, 1–8, https://doi.org/10.1057/rm.2009.17, 2010.

Fischer, E. M., Seneviratne, S. I., Vidale, P. L., Lüthi, D., and Schär, C.: Soil Moisture–Atmosphere Interactions during the 2003 European Summer Heat Wave, Journal of Climate, 20, 5081–5099, https://doi.org/10.1175/JCLI4288.1, 2007.

Fischer, E. M., Sippel, S., and Knutti, R.: Increasing probability of record-shattering climate extremes, Nature Climate Change, 11, 689–695, https://doi.org/10.1038/s41558-021-01092-9, 2021.

Fischer, E. M., Beyerle, U., Bloin-Wibe, L., Gessner, C., Humphrey, V., Lehner, F., Pendergrass, A. G., Sippel, S., Zeder, J., and Knutti, R.: Storylines for unprecedented heatwaves based on ensemble boosting, Nature Communications, 14, 4643, https://doi.org/10.1038/s41467-023-40112-4, 2023.

Fischer, E. M., Bador, M., Huser, R., Kendon, E. J., Robinson, A., and Sippel, S.: Record-breaking extremes in a warming climate, Nature Reviews Earth & Environment, pp. 1–15, https://doi.org/10.1038/s43017-025-00681-y, 2025.

Fix-Hewitt, F., Zeileis, A., Stucke, I., Stauffer, R., and Mayr, G. J.: Properties and characteristics of atmospheric deserts over Europe: a first statistical analysis, Weather and Climate Dynamics, 7, 17–35, https://doi.org/10.5194/wcd-7-17-2026, 2026.

Fleishman, E., Rupp, D. E., Loikith, P. C., Bumbaco, K. A., and O'Neill, L. W.: Synthesis of Publications on the Anomalous June 2021 Heat Wave in the Pacific Northwest of the United States and Canada, Bulletin of the American Meteorological Society, 106, E1155–E1174, https://doi.org/10.1175/BAMS-D-24-0188.1, 2025.

García-Herrera, R., Díaz, J., Trigo, R. M., Luterbacher, J., and Fischer, E. M.: A Review of the European Summer Heat Wave of 2003, Critical Reviews in Environmental Science and Technology, 40, 267–306, https://doi.org/10.1080/10643380802238137, 2010.

https://doi.org/10.5194/egusphere-2026-2005
Preprint. Discussion started: 28 April 2026

Gessner, C., Fischer, E. M., Beyerle, U., and Knutti, R.: Very Rare Heat Extremes: Quantifying and Understanding Using Ensemble Reinitialization, Journal of Climate, 34, 6619–6634, https://doi.org/10.1175/JCLI-D-20-0916.1, 2021.

Giardina, C., Kurchan, J., Lecomte, V., and Tailleur, J.: Simulating Rare Events in Dynamical Processes, Journal of Statistical Physics, 145, 787–811, https://doi.org/10.1007/s10955-011-0350-4, 2011.

Goodwin, P. and Wright, G.: The limits of forecasting methods in anticipating rare events, Technological Forecasting and Social Change, 77, 355–368, https://doi.org/10.1016/j.techfore.2009.10.008, 2010.

Green, J. S. A.: The Weather During July 1976: Some Dynamical Considerations of the Drought, Weather, 32, 120–126, https://doi.org/10.1002/j.1477-8696.1977.tb04532.x, 1977.

Hazeleger, W., van den Hurk, B. J. J. M., Min, E., van Oldenborgh, G. J., Petersen, A. C., Stainforth, D. A., Vasileiadou, E., and Smith, L. A.: Tales of future weather, Nature Climate Change, 5, 107–113, https://doi.org/10.1038/nclimate2450, 2015.

Hersbach, H., Bell, B., Berrisford, P., Hirahara, S., Horányi, A., Muñoz-Sabater, J., Nicolas, J., Peubey, C., Radu, R., Schepers, D., Simmons, A., Soci, C., Abdalla, S., Abellan, X., Balsamo, G., Bechtold, P., Biavati, G., Bidlot, J., Bonavita, M., De Chiara, G., Dahlgren, P., Dee, D., Diamantakis, M., Dragani, R., Flemming, J., Forbes, R., Fuentes, M., Geer, A., Haimberger, L., Healy, S., Hogan, R. J., Hólm, E., Janisková, M., Keeley, S., Laloyaux, P., Lopez, P., Lupu, C., Radnoti, G., de Rosnay, P., Rozum, I., Vamborg, F., Villaume, S., and Thépaut, J.-N.: The ERA5 global reanalysis, Quarterly Journal of the Royal Meteorological Society, 146, 1999–2049, https://doi.org/10.1002/qj.3803, 2020.

Hersbach, H., Bell, B., Berrisford, P., Biavati, G., Horányi, A., Muñoz Sabater, J., Nicolas, J., Peubey, C., Radu, R., Rozum, I., Schepers, D., Simmons, A., Soci, C., Dee, D., and Thépaut, J.-N.: ERA5 hourly data on pressure levels from 1940 to present, https://doi.org/10.24381/cds.bd0915c6, 2023a.

Hersbach, H., Bell, B., Berrisford, P., Biavati, G., Horányi, A., Muñoz Sabater, J., Nicolas, J., Peubey, C., Radu, R., Rozum, I., Schepers, D., Simmons, A., Soci, C., Dee, D., and Thépaut, J.-N.: ERA5 hourly data on single levels from 1940 to present, https://doi.org/10.24381/cds.adbb2d47, 2023b.

Hotz, B., Papritz, L., and Röthlisberger, M.: Understanding the vertical temperature structure of recent record-shattering heatwaves, Weather and Climate Dynamics, 5, 323–343, https://doi.org/10.5194/wcd-5-323-2024, 2024.

Kautz, L.-A., Martius, O., Pfahl, S., Pinto, J. G., Ramos, A. M., Sousa, P. M., and Woollings, T.: Atmospheric blocking and weather extremes over the Euro-Atlantic sector – a review, Weather and Climate Dynamics, 3, 305–336, https://doi.org/10.5194/wcd-3-305-2022, 2022.

Kelder, T., Marjoribanks, T. I., Slater, L. J., Prudhomme, C., Wilby, R. L., Wagemann, J., and Dunstone, N.: An open workflow to gain insights about low-likelihood high-impact weather events from initialized predictions, Meteorological Applications, 29, e2065, https://doi.org/10.1002/met.2065, 2022a.

Kelder, T., Wanders, N., van der Wiel, K., Marjoribanks, T. I., Slater, L. J., Wilby, R. l., and Prudhomme, C.: Interpreting extreme climate impacts from large ensemble simulations—are they unseen or unrealistic?, Environmental Research Letters, 17, 044 052, https://doi.org/10.1088/1748-9326/ac5cf4, 2022b.

Kelder, T., Heinrich, D., Klok, L., Thompson, V., Goulart, H. M. D., Hawkins, E., Slater, L. J., Suarez-Gutierrez, L., Wilby, R. L., Coughlan de Perez, E., Stephens, E. M., Burt, S., van den Hurk, B., de Vries, H., van der Wiel, K., Schipper, E. L. F., Carmona Baéz, A., van Bueren, E., and Fischer, E. M.: How to stop being surprised by unprecedented weather, Nature Communications, 16, 1–15, https://doi.org/10.1038/s41467-025-57450-0, 2025.

https://doi.org/10.5194/egusphere-2026-2005
Preprint. Discussion started: 28 April 2026

Kendon, E. J., Ciavarella, A., McCarthy, M., Brown, S., Christidis, N., Kay, G., Dunstone, N., Fereday, D., and Pope, J. O.: Multiperspective view of the 1976 drought–heatwave event and its changing likelihood, Quarterly Journal of the Royal Meteorological Society, 150, 232–261, https://doi.org/10.1002/qj.4594, 2024.

Kornhuber, K., Osprey, S., Coumou, D., Petri, S., Petoukhov, V., Rahmstorf, S., and Gray, L.: Extreme weather events in early summer 2018 connected by a recurrent hemispheric wave-7 pattern, Environmental Research Letters, 14, 054 002, https://doi.org/10.1088/1748-9326/ab13bf, 2019.

Le Tertre, A., Lefranc, A., Eilstein, D., Declercq, C., Medina, S., Blanchard, M., Chardon, B., Fabre, P., Filleul, L., Jusot, J.-F., Pascal, L., Prouvost, H., Cassadou, S., and Ledrans, M.: Impact of the 2003 Heatwave on All-Cause Mortality in 9 French Cities, Epidemiology, 17, 75, https://doi.org/10.1097/01.ede.0000187650.36636.1f, 2006.

Liu, P., Reed, K. A., Garner, S. T., Zhao, M., and Zhu, Y.: Blocking Simulations in GFDL GCMs for CMIP5 and CMIP6, Journal of Climate, 35, 5053–5070, https://doi.org/10.1175/JCLI-D-21-0456.1, 2022.

Lüthi, S., Huber, V., Pascal, M., Beyerle, U., Pyrina, M., Domeisen, D., Vicedo-Cabrera, A. M., and Fischer, E.: Storylines for month-long heatwaves and associated heat-related mortality impacts over Western Europe, https://doi.org/10.21203/rs.3.rs-5356341/v1, 2024.

Mahesh, A., Collins, W., Bonev, B., Brenowitz, N., Cohen, Y., Elms, J., Harrington, P., Kashinath, K., Kurth, T., North, J., OBrien, T., Pritchard, M., Pruitt, D., Risser, M., Subramanian, S., and Willard, J.: Huge Ensembles Part I: Design of Ensemble Weather Forecasts using Spherical Fourier Neural Operators, https://doi.org/10.48550/arXiv.2408.03100, arXiv:2408.03100 [physics], 2025a.

Mahesh, A., Collins, W., Bonev, B., Brenowitz, N., Cohen, Y., Harrington, P., Kashinath, K., Kurth, T., North, J., OBrien, T., Pritchard, M., Pruitt, D., Risser, M., Subramanian, S., and Willard, J.: Huge Ensembles Part II: Properties of a Huge Ensemble of Hindcasts Generated with Spherical Fourier Neural Operators, https://doi.org/10.48550/arXiv.2408.01581, arXiv:2408.01581 [cs], 2025b.

Muñoz-Sabater, J.: ERA5-Land monthly averaged data from 1950 to present., https://doi.org/10.24381/cds.68d2bb30, 2019.

Muñoz-Sabater, J., Dutra, E., Agustí-Panareda, A., Albergel, C., Arduini, G., Balsamo, G., Boussetta, S., Choulga, M., Harrigan, S., Hersbach, H., Martens, B., Miralles, D. G., Piles, M., Rodríguez-Fernández, N. J., Zsoter, E., Buontempo, C., and Thépaut, J.-N.: ERA5-Land: a state-of-the-art global reanalysis dataset for land applications, Earth System Science Data, 13, 4349–4383, https://doi.org/10.5194/essd-13-4349-2021, 2021.

Nordmann, A.: (Im)Plausibility2, International Journal of Foresight and Innovation Policy, 9, 125–132, https://doi.org/10.1504/IJFIP.2013.058612, 2013.

Noyelle, R., Caubel, A., Meurdesoif, Y., Faranda, D., and Yiou, P.: Evolution of the Dynamics of Centennial Hot Summers in Western Europe With Climate Change, Geophysical Research Letters, 52, e2025GL115 552, https://doi.org/10.1029/2025GL115552, 2025a.

Noyelle, R., Caubel, A., Meurdesoif, Y., Yiou, P., and Faranda, D.: Statistical and Dynamical Aspects of Extremely Hot Summers in Western Europe Sampled with a Rare Event Algorithm, Journal of Climate, 38, 4763–4787, https://doi.org/10.1175/JCLI-D-24-0635.1, 2025b.

Pappert, D., Tuel, A., Coumou, D., Vrac, M., and Martius, O.: Long vs. short: understanding the dynamics of persistent summer hot spells in Europe, Weather and Climate Dynamics, 6, 769–788, https://doi.org/10.5194/wcd-6-769-2025, 2025.

Philip, S., Kew, S., van Oldenborgh, G. J., Otto, F., Vautard, R., van der Wiel, K., King, A., Lott, F., Arrighi, J., Singh, R., and van Aalst, M.: A protocol for probabilistic extreme event attribution analyses, Advances in Statistical Climatology, Meteorology and Oceanography, 6, 177–203, https://doi.org/10.5194/ascmo-6-177-2020, 2020.

Pitkänen, M. R. A., Mikkonen, S., Lehtinen, K. E. J., Lipponen, A., and Arola, A.: Artificial bias typically neglected in comparisons of uncertain atmospheric data, Geophysical Research Letters, 43, 10,003–10,011, https://doi.org/10.1002/2016GL070852, 2016.

https://doi.org/10.5194/egusphere-2026-2005
Preprint. Discussion started: 28 April 2026

Polt, K. D., Ward, P. J., De Ruiter, M., Bogdanovich, E., Reichstein, M., Frank, D., and Orth, R.: Quantifying impact-relevant heatwave durations, Environmental Research Letters, 18, 104 005, https://doi.org/10.1088/1748-9326/acf05e, 2023.

Ragone, F. and Bouchet, F.: Rare Event Algorithm Study of Extreme Warm Summers and Heatwaves Over Europe, Geophysical Research Letters, 48, e2020GL091 197, https://doi.org/10.1029/2020GL091197, 2021.

Ragone, F., Wouters, J., and Bouchet, F.: Computation of extreme heat waves in climate models using a large deviation algorithm, Proceedings of the National Academy of Sciences, 115, 24–29, https://doi.org/10.1073/pnas.1712645115, 2018.

Rebetez, M., Dupont, O., and Giroud, M.: An analysis of the July 2006 heatwave extent in Europe compared to the record year of 2003, Theoretical and Applied Climatology, 95, 1–7, https://doi.org/10.1007/s00704-007-0370-9, 2009.

Robine, J.-M., Cheung, S. L. K., Roy, S. L., Oyen, H. V., Griffiths, C., Michel, J.-P., and Herrmann, F. R.: Death toll exceeded 70,000 in Europe during the summer of 2003, Comptes Rendus. Biologies, 331, 171–178, https://doi.org/10.1016/j.crvi.2007.12.001, 2007.

Rodda, J. C. and Marsh, T. J.: The 1975-76 Drought - a contemporary and retrospective review, National Hydrological Monitoring Programme series, http://www.ceh.ac.uk/data/nrfa/nhmp/other_reports/CEH_1975-76_Drought_Report_Rodda_and_Marsh.pdf, iSBN: 9781906698249 Num Pages: 58, 2011.

Rodgers, K. B., Lee, S.-S., Rosenbloom, N., Timmermann, A., Danabasoglu, G., Deser, C., Edwards, J., Kim, J.-E., Simpson, I. R., Stein, K., Stuecker, M. F., Yamaguchi, R., Bódai, T., Chung, E.-S., Huang, L., Kim, W. M., Lamarque, J.-F., Lombardozzi, D. L., Wieder, W. R., and Yeager, S. G.: Ubiquity of human-induced changes in climate variability, Earth System Dynamics, 12, 1393–1411, https://doi.org/10.5194/esd-12-1393-2021, 2021.

Roemer, F. E., Fischer, E., Noyelle, R., and Knutti, R.: Supplementary code for "Assessing the plausibility of unprecedented events: A process-based approach applied to month-long heatwaves in Western Europe", https://doi.org/10.5281/zenodo.19492889, 2026a.

Roemer, F. E., Fischer, E., Noyelle, R., and Knutti, R.: Supplementary data for "Assessing the plausibility of unprecedented events: A process-based approach applied to month-long heatwaves in Western Europe", https://doi.org/10.5281/zenodo.19494785, 2026b.

Russo, S., Sillmann, J., and Fischer, E. M.: Top ten European heatwaves since 1950 and their occurrence in the coming decades, Environmental Research Letters, 10, 124 003, https://doi.org/10.1088/1748-9326/10/12/124003, 2015.

Röthlisberger, M. and Martius, O.: Quantifying the Local Effect of Northern Hemisphere Atmospheric Blocks on the Persistence of Summer Hot and Dry Spells, Geophysical Research Letters, 46, 10 101–10 111, https://doi.org/10.1029/2019GL083745, 2019.

Röthlisberger, M., Frossard, L., Bosart, L. F., Keyser, D., and Martius, O.: Recurrent Synoptic-Scale Rossby Wave Patterns and Their Effect on the Persistence of Cold and Hot Spells, Journal of Climate, 32, 3207–3226, https://doi.org/10.1175/JCLI-D-18-0664.1, 2019.

Röthlisberger, M., Sprenger, M., Flaounas, E., Beyerle, U., and Wernli, H.: The substructure of extremely hot summers in the Northern Hemisphere, Weather and Climate Dynamics, 1, 45–62, https://doi.org/10.5194/wcd-1-45-2020, 2020.

Röthlisberger, M., Sprenger, M., Beyerle, U., Fischer, E. M., and Wernli, H.: Advective, adiabatic and diabatic contributions to heat extremes simulated with the Community Earth System Model version 2, EGUsphere, pp. 1–32, https://doi.org/10.5194/egusphere-2025-5146, 2025.

Schulzweida, U.: CDO User Guide, https://doi.org/10.5281/zenodo.10020800, 2023.

Schumacher, D. L., Singh, J., Hauser, M., Fischer, E. M., Wild, M., and Seneviratne, S. I.: Exacerbated summer European warming not captured by climate models neglecting long-term aerosol changes, Communications Earth & Environment, 5, 182, https://doi.org/10.1038/s43247-024-01332-8, 2024.

Selin, C.: Trust and the illusive force of scenarios, Futures, 38, 1–14, https://doi.org/10.1016/j.futures.2005.04.001, 2006.

Selin, C. and Guimarães Pereira, A.: Pursuing plausibility, International Journal of Foresight and Innovation Policy, 9, 93–109, https://doi.org/10.1504/IJFIP.2013.058616, 2013.

https://doi.org/10.5194/egusphere-2026-2005
Preprint. Discussion started: 28 April 2026

Seneviratne, S. I., Koster, R. D., Guo, Z., Dirmeyer, P. A., Kowalczyk, E., Lawrence, D., Liu, P., Mocko, D., Lu, C.-H., Oleson, K. W., and Verseghy, D.: Soil Moisture Memory in AGCM Simulations: Analysis of Global Land–Atmosphere Coupling Experiment (GLACE) Data, Journal of Hydrometeorology, 7, 1090–1112, https://doi.org/10.1175/JHM533.1, 2006.

Seneviratne, S. I., Corti, T., Davin, E. L., Hirschi, M., Jaeger, E. B., Lehner, I., Orlowsky, B., and Teuling, A. J.: Investigating soil moisture–climate interactions in a changing climate: A review, Earth-Science Reviews, 99, 125–161, https://doi.org/10.1016/j.earscirev.2010.02.004, 2010.

Shepherd, T. G., Boyd, E., Calel, R. A., Chapman, S. C., Dessai, S., Dima-West, I. M., Fowler, H. J., James, R., Maraun, D., Martius, O., Senior, C. A., Sobel, A. H., Stainforth, D. A., Tett, S. F. B., Trenberth, K. E., van den Hurk, B. J. J. M., Watkins, N. W., Wilby, R. L., and Zenghelis, D. A.: Storylines: an alternative approach to representing uncertainty in physical aspects of climate change, Climatic Change, 151, 555–571, https://doi.org/10.1007/s10584-018-2317-9, 2018.

Sillmann, J., Shepherd, T. G., van den Hurk, B., Hazeleger, W., Martius, O., Slingo, J., and Zscheischler, J.: Event-Based Storylines to Address Climate Risk, Earth's Future, 9, e2020EF001 783, https://doi.org/10.1029/2020EF001783, 2021.

Singh, J., Sippel, S., and Fischer, E. M.: Circulation dampened heat extremes intensification over the Midwest USA and amplified over Western Europe, Communications Earth & Environment, 4, 432, https://doi.org/10.1038/s43247-023-01096-7, 2023.

Suarez-Gutierrez, L., Müller, W. A., Li, C., and Marotzke, J.: Dynamical and thermodynamical drivers of variability in European summer heat extremes, Climate Dynamics, 54, 4351–4366, https://doi.org/10.1007/s00382-020-05233-2, 2020.

Suarez-Gutierrez, L., Beyerle, U., Mittermeier, M., Vautard, R., and Fischer, E.: Worst-Case European Heat and Drought Storylines generated using Ensemble Boosting, https://doi.org/10.21203/rs.3.rs-7113183/v1, iSSN: 2693-5015, 2025.

Sánchez-Benítez, A., Goessling, H., Pithan, F., Semmler, T., and Jung, T.: The July 2019 European Heat Wave in a Warmer Climate: Storyline Scenarios with a Coupled Model Using Spectral Nudging, Journal of Climate, 35, 2373–2390, https://doi.org/10.1175/JCLI-D-21-0573.1, 2022.

Thompson, V., Dunstone, N. J., Scaife, A. A., Smith, D. M., Slingo, J. M., Brown, S., and Belcher, S. E.: High risk of unprecedented UK rainfall in the current climate, Nature Communications, 8, 107, https://doi.org/10.1038/s41467-017-00275-3, 2017.

Thompson, V., Dunstone, N. J., Scaife, A. A., Smith, D. M., Hardiman, S. C., Ren, H.-L., Lu, B., and Belcher, S. E.: Risk and dynamics of unprecedented hot months in South East China, Climate Dynamics, 52, 2585–2596, https://doi.org/10.1007/s00382-018-4281-5, 2019.

Thompson, V., Mitchell, D., Hegerl, G. C., Collins, M., Leach, N. J., and Slingo, J. M.: The most at-risk regions in the world for high-impact heatwaves, Nature Communications, 14, 2152, https://doi.org/10.1038/s41467-023-37554-1, 2023.

Tibaldi, S. and Molteni, F.: On the operational predictability of blocking, Tellus A, 42, 343–365, https://doi.org/10.1034/j.1600-0870.1990.t01-2-00003.x, _eprint: https://onlinelibrary.wiley.com/doi/pdf/10.1034/j.1600-0870.1990.t01-2-00003.x, 1990.

Tuel, A. and Martius, O.: Weather persistence on sub-seasonal to seasonal timescales: a methodological review, Earth System Dynamics, 14, 955–987, https://doi.org/10.5194/esd-14-955-2023, 2023.

Urueña, S.: Understanding "plausibility": A relational approach to the anticipatory heuristics of future scenarios, Futures, 111, 15–25, https://doi.org/10.1016/j.futures.2019.05.002, 2019.

van den Brink, H. W., Können, G. P., Opsteegh, J. D., van Oldenborgh, G. J., and Burgers, G.: Estimating return periods of extreme events from ECMWF seasonal forecast ensembles, International Journal of Climatology, 25, 1345–1354, https://doi.org/10.1002/joc.1155, 2005.

van den Hurk, B. J. J. M., Baldissera Pacchetti, M., Boere, E., Ciullo, A., Coulter, L., Dessai, S., Ercin, E., Goulart, H. M. D., Hamed, R., Hochrainer-Stigler, S., Koks, E., Kubiczek, P., Levermann, A., Mechler, R., van Meersbergen, M., Mester, B., Middelanis, R., Minderhoud, K., Mysiak, J., Nirandjan, S., van den Oord, G., Otto, C., Sayers, P., Schewe, J., Shepherd, T. G., Sillmann, J., Stuparu, D., Vogt, T., and

https://doi.org/10.5194/egusphere-2026-2005
Preprint. Discussion started: 28 April 2026

Witpas, K.: Climate impact storylines for assessing socio-economic responses to remote events, Climate Risk Management, 40, 100 500, https://doi.org/10.1016/j.crm.2023.100500, 2023.

van der Helm, R.: Towards a clarification of probability, possibility and plausibility: how semantics could help futures practice to improve, Foresight, 8, 17–27, https://doi.org/10.1108/14636680610668045, 2006.

van der Wiel, K., Lenderink, G., and de Vries, H.: Physical storylines of future European drought events like 2018 based on ensemble climate modelling, Weather and Climate Extremes, 33, 100 350, https://doi.org/10.1016/j.wace.2021.100350, 2021.

Vautard, R., Christidis, N., Ciavarella, A., Alvarez-Castro, C., Bellprat, O., Christiansen, B., Colfescu, I., Cowan, T., Doblas-Reyes, F., Eden, J., Hauser, M., Hegerl, G., Hempelmann, N., Klehmet, K., Lott, F., Nangini, C., Orth, R., Radanovics, S., Seneviratne, S. I., van Oldenborgh, G. J., Stott, P., Tett, S., Wilcox, L., and Yiou, P.: Evaluation of the HadGEM3-A simulations in view of detection and attribution of human influence on extreme events in Europe, Climate Dynamics, 52, 1187–1210, https://doi.org/10.1007/s00382-018-4183-6, 2019.

Vautard, R., Cattiaux, J., Happé, T., Singh, J., Bonnet, R., Cassou, C., Coumou, D., D'Andrea, F., Faranda, D., Fischer, E., Ribes, A., Sippel, S., and Yiou, P.: Heat extremes in Western Europe increasing faster than simulated due to atmospheric circulation trends, Nature Communications, 14, 6803, https://doi.org/10.1038/s41467-023-42143-3, 2023.

Vogel, M. M., Zscheischler, J., and Seneviratne, S. I.: Varying soil moisture–atmosphere feedbacks explain divergent temperature extremes and precipitation projections in central Europe, Earth System Dynamics, 9, 1107–1125, https://doi.org/10.5194/esd-9-1107-2018, 2018.

White, R. H., Anderson, S., Booth, J. F., Braich, G., Draeger, C., Fei, C., Harley, C. D. G., Henderson, S. B., Jakob, M., Lau, C.-A., Mareshet Admasu, L., Narinesingh, V., Rodell, C., Roocroft, E., Weinberger, K. R., and West, G.: The unprecedented Pacific Northwest heatwave of June 2021, Nature Communications, 14, 727, https://doi.org/10.1038/s41467-023-36289-3, 2023.

Whittaker, T. and Di Luca, A.: Constructing extreme heatwave storylines with differentiable climate models, Weather and Climate Dynamics, 7, 393–410, https://doi.org/10.5194/wcd-7-393-2026, 2026.

Wilson, I.: Mental maps of the future: an intuitive logics approach to scenarios, Learning from the future: Competitive foresight scenarios, pp. 81–108, 1998.

World Meteorological Organization (WMO), Programme of the European Union, Copernicus Climate Change Service (C3S), and European Centre for Medium-Range Weather Forecasts (ECMWF): European State of the Climate – Report 2024, https://library.wmo.int/records/item/69475-european-state-of-the-climate-report-2024?language_id=13&back=&offset=, 2025.

Yiou, P., Cadiou, C., Faranda, D., Jézéquel, A., Malhomme, N., Miloshevich, G., Noyelle, R., Pons, F., Robin, Y., and Vrac, M.: Ensembles of climate simulations to anticipate worst case heatwaves during the Paris 2024 Olympics, npj Climate and Atmospheric Science, 6, 188, https://doi.org/10.1038/s41612-023-00500-5, 2023.

Zschenderlein, P., Fink, A. H., Pfahl, S., and Wernli, H.: Processes determining heat waves across different European climates, Quarterly Journal of the Royal Meteorological Society, 145, 2973–2989, https://doi.org/10.1002/qj.3599, 2019.

Zuo, J., Pullen, S., Palmer, J., Bennetts, H., Chileshe, N., and Ma, T.: Impacts of heat waves and corresponding measures: a review, Journal of Cleaner Production, 92, 1–12, https://doi.org/10.1016/j.jclepro.2014.12.078, 2015.